Neutron Radiography and Tomography

Eberhard H. Lehmann

Paul Scherrer Institut, CH-5232 Villigen
Spallation Neutron Source Division (ASQ)
Neutron Imaging & Activation

Outline (1)

1. How transmission imaging started
2. Neutron interaction, comparison to X-ray
3. What means neutron imaging today
4. Facilities for neutron imaging
5. Detector options for digital neutron imaging
6. Limitations and application range

Outline (2)

7. **Specific methods in neutron imaging**

8. **Principles of neutron tomography**

9. **Typical applications of neutron imaging**

- Science
- Industry
- Cultural heritage

7. **Future trends and aspects**

How transmission imaging started

X-ray

First experiments with a new kind of radiation were performed by **Konrad Röntgen** in **1895** during investigations with cathode-ray tubes.

He found the new ray could pass through most substances casting shadows of solid objects.

In conjunction with a photographic plate, a picture of interior body parts can be obtained when human tissue will be investigated.

One of the first experiments late in 1895 was a film of a hand of his wife.

The bones and also finger rings deliver much higher contrast than the soft tissue.

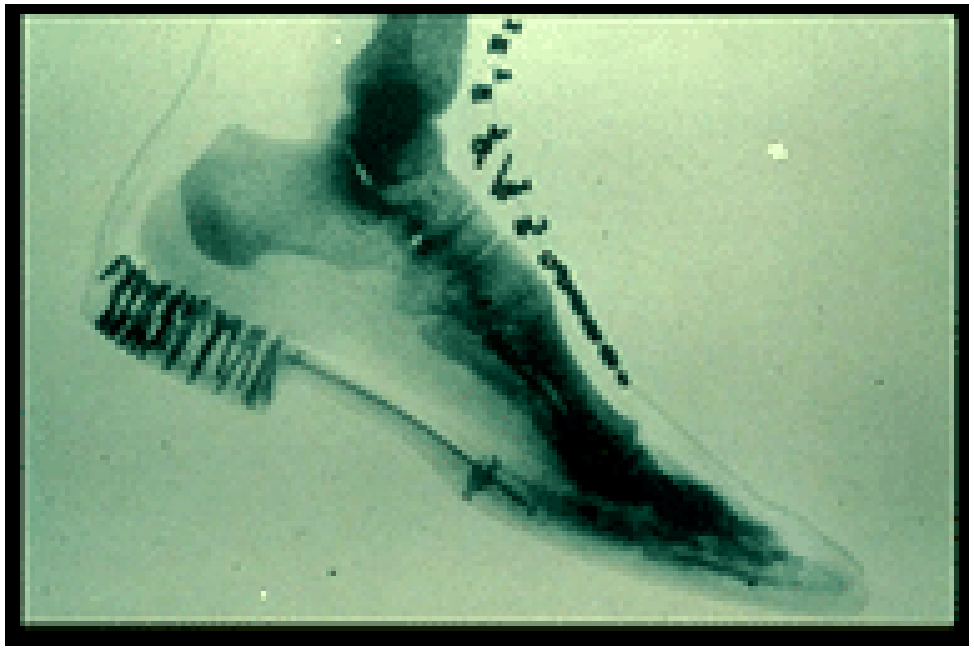

Some more exotic applications of X-ray transmission in the earlier period of use.

Such an “open” laboratory wouldn’t be tolerated today due to radiation protection regulations!

Only few month later (**1896**)
Henri Becquerel discovered the natural radioactivity when he investigated the fluorescence behavior of uranium salts and found films blackened through their light tight covers.

Gamma radiography became first not as popular as X-ray one due to the availability of the suited source materials.

The discovery of Radium and artificial radioactive gamma sources (Co, Ir, Cs) broadened the application.

Gamma radiation

During World War II, industrial radiography grew tremendously as part of the Navy's shipbuilding and submarine program.

Roots of neutron radiography

Taken from C.O. Fischer's article in WCNR-4

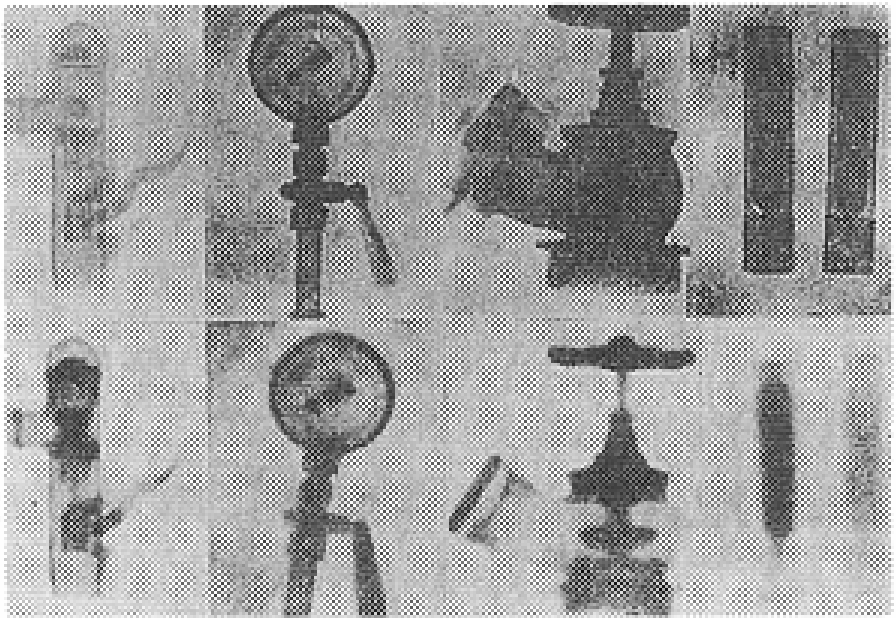

As typical: valves, manometers, injectors

Berlin, 1935 – 1938
H. Kallmann & Kuhn with Ra-Be and neutron generator

Berlin until Dec. 1944
O. Peter with an accelerator neutron source

But the real programs with neutrons started after World War II at research reactors

From X-rays to neutrons

Nuclear Interactions

- X-rays interact with the electron shell of the atoms by Compton scattering, photo-effect and pair-production
- Thermal neutrons interact with the atomic nuclei by collision (elastic and inelastic scattering), capture and (seldom) fission

Periodisches System der Elemente

1a	2a	3b	4b	5b	6b	7b	8			1b	2b	3a	4a	5a	6a	7a	0
H																	He
Li	Be											B	C	N	O	F	Ne
Na	Mg											Al	Si	P	S	Cl	Ar
K	Ca	Sc	Ti	V	Cr	Mn	Fe	Co	Ni	Cu	Zn	Ga	Ge	As	Se	Br	Kr
Rb	Sr	Y	Zr	Nb	Mo	Tc	Ru	Rh	Pd	Ag	Cd	In	Sn	Sb	Te	I	Xe
Cs	Ba	La	Hf	Ta	W	Re	Os	Ir	Pt	Au	Hg	Tl	Pb	Bi	Po	At	Rn
Fr	Ra	Ac	Rf	Ha													

*Lanthanides	Ce	Pr	Nd	Pm	Sm	Eu	Gd	Tb	Dy	Ho	Er	Tm	Yb	Lu
**Actinides	Th	Pa	U	Np	Pu	Am	Cm	Bk	Cf	Es	Fm	Md	No	

Attenuation coefficients with X-ray [cm?^{1}]

1a	2a	3b	4b	5b	6b	7b	8			1b	2b	3a	4a	5a	6a	7a	0
H 0.02																	He 0.02
Li 0.06	Be 0.22											B 0.28	C 0.27	N 0.11	O 0.16	F 0.14	Ne 0.17
Na 0.13	Mg 0.24											Al 0.38	Si 0.33	P 0.25	S 0.30	Cl 0.23	Ar 0.20
K 0.14	Ca 0.26	Sc 0.48	Ti 0.73	V 1.04	Cr 1.29	Mn 1.32	Fe 1.57	Co 1.78	Ni 1.96	Cu 1.97	Zn 1.64	Ga 1.42	Ge 1.33	As 1.50	Se 1.23	Br 0.90	Kr 0.73
Rb 0.47	Sr 0.86	Y 1.61	Zr 2.47	Nb 3.43	Mo 4.29	Tc 5.06	Ru 5.71	Rh 6.08	Pd 6.13	Ag 5.67	Cd 4.84	In 4.31	Sn 3.98	Sb 4.28	Te 4.06	I 3.45	Xe 2.53
Cs 1.42	Ba 2.73	La 5.04	Hf 19.70	Ta 25.47	W 30.49	Re 34.47	Os 37.92	Ir 39.01	Pt 38.61	Au 35.94	Hg 25.88	Tl 23.23	Pb 22.81	Bi 20.28	Po 20.22	At	Rn 9.77
Fr	Ra 11.80	Ac 24.47	Rf	Ha													

Lanthanides	Ce 5.79	Pr 6.23	Nd 6.46	Pm 7.33	Sm 7.68	Eu 5.66	Gd 8.69	Tb 9.46	Dy 10.17	Ho 10.91	Er 11.70	Tm 12.49	Yb 9.32	Lu 14.07
*Actinides	Th 28.95	Pa 39.65	U 49.08	Np	Pu	Am	Cm	Bk	Vf	Es	Fm	Md	No	Lr x-ray

X-ray

Legend

Attenuation coefficient [cm?^{1}] = sp.gr. * μ/δ

sp.gr.: Handbook of Chemistry and Physics, 56th Edition 1975-1976.

μ/δ: J. H. Hubbell[+] and S. M. Seltzer Ionizing Radiation Division, Physics Laboratory National Institute of Standards and Technology Gaithersburg, MD 20899, http://physics.nist.gov/PhysRefData/XrayMassCoef/tab3.html.

Attenuation coefficients with neutrons [cm?$^{-1}$]

1a	2a	3b	4b	5b	6b	7b	8			1b	2b	3a	4a	5a	6a	7a	0
H 3.44																	He 0.02
Li 3.30	Be 0.79											B 101.60	C 0.56	N 0.43	O 0.17	F 0.20	Ne 0.10
Na 0.09	Mg 0.15											Al 0.10	Si 0.11	P 0.12	S 0.06	Cl 1.33	Ar 0.03
K 0.06	Ca 0.08	Sc 2.00	Ti 0.60	V 0.72	Cr 0.54	Mn 1.21	Fe 1.19	Co 3.92	Ni 2.05	Cu 1.07	Zn 0.35	Ga 0.49	Ge 0.47	As 0.67	Se 0.73	Br 0.24	Kr 0.61
Rb 0.08	Sr 0.14	Y 0.27	Zr 0.29	Nb 0.40	Mo 0.52	Tc 1.76	Ru 0.58	Rh 10.88	Pd 0.78	Ag 4.04	Cd 115.11	In 7.58	Sn 0.21	Sb 0.30	Te 0.25	I 0.23	Xe 0.43
Cs 0.29	Ba 0.07	La 0.52	Hf 4.99	Ta 1.49	W 1.47	Re 6.85	Os 2.24	Ir 30.46	Pt 1.46	Au 6.23	Hg 16.21	Tl 0.47	Pb 0.38	Bi 0.27	Po	At	Rn
Fr	Ra 0.34	Ac	Rf	Ha													
*Lanthanides	Ce 0.14	Pr 0.41	Nd 1.87	Pm 5.72	Sm 171.47	Eu 94.58	Gd 1479.04	Tb 0.93	Dy 32.42	Ho 2.25	Er 5.48	Tm 3.53	Yb 1.40	Lu 2.75			
**Actinides	Th 0.59	Pa 8.46	U 0.82	Np 9.80	Pu 50.20	Am 2.86	Cm	Bk	Cf	Es	Fm	Md	No	Lr neut.			

thermal neutrons

Legend

$$\text{Attenuation coefficient [cm?}^{-1}\text{]} = \frac{\sigma\text{-total} * \text{sp.gr.} * 0.6023}{\text{at.wt.}}$$

σ-total: JEF Report 14, TABLE OF SIMPLE INTEGRAL NEUTRON CROSS SECTION DATA FROM JEF-2.2, ENDF/B-VI, JENDL-3.2, BROND-2 AND CENDL-2, AEN NEA, 1994.
and Special Feature: Neutron scattering lengths and cross sections, Varley F. Sears, AECL Research, Chalk River Laboratories Chalk River, Ontario, Canada KOJ 1JO, Neutron News, Vol. 3, 1992, http://www.ncnr.nist.gov/resources/n-lengths/list.html.

sp.gr.: Handbook of Chemistry and Physics, 56th Edition 1975-1976.

at.wt.: Handbook of Chemistry and Physics, 56th Edition 1975-1976.

Comparison between the interaction probabilities for (thermal) neutrons and x-ray

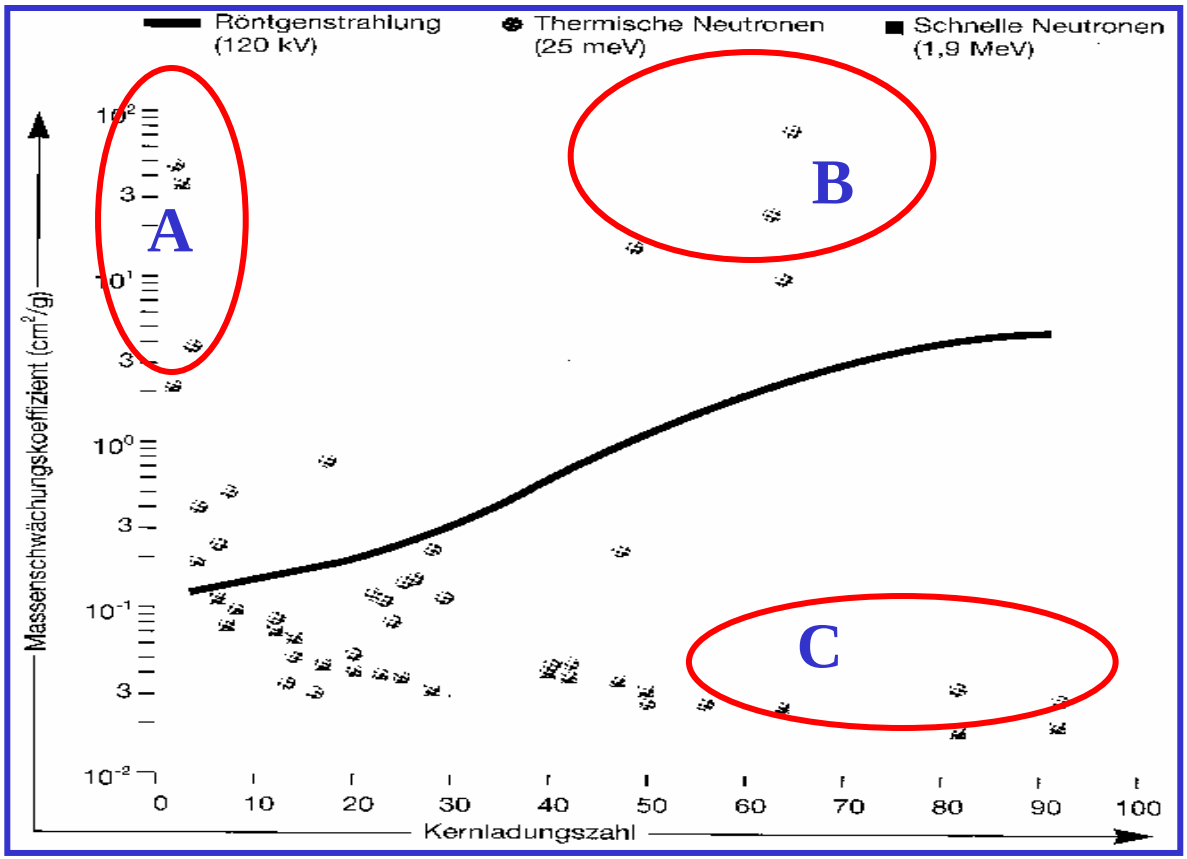

The deviations in the cross-sections are especially high for:
A: light materials like hydrogen
B: especially strong neutron absorbers Gd, Cd, Dy, In
C: heavy materials like Pb, Bi, U , Th

Comparison of transmission images

HARD DRIVE

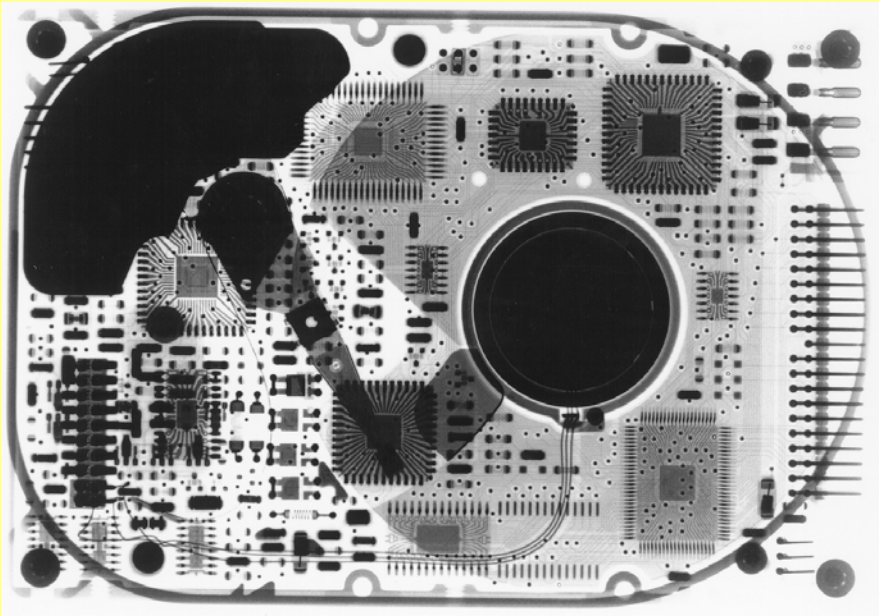

X-ray

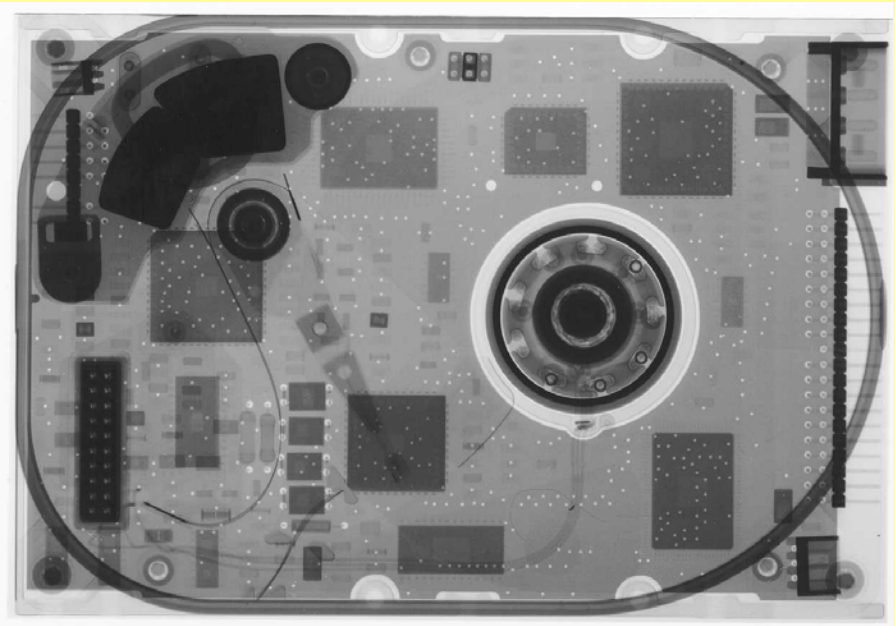

neutron

high contrast for metals
no contrast for plastics

metals are more transparent
high contrast for plastics

Simplified setup of a radiography facility

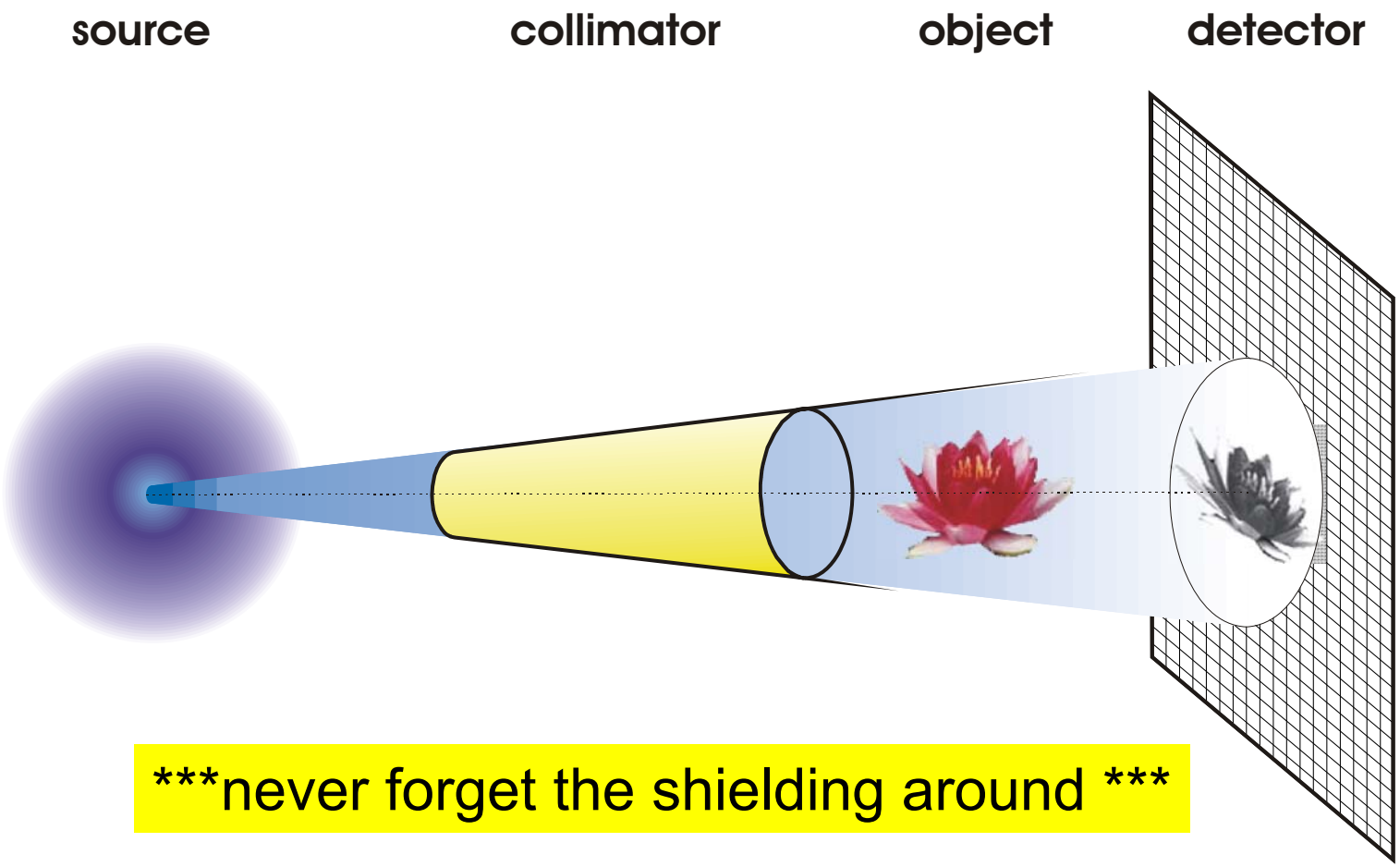

***never forget the shielding around ***

Neutron sources

- Research reactor (ILL, FRM-2,...)
- Spallation sources (ISIS, SINQ, SNS,...)
- Radioactive nuclides (Cf, Ra-Be, Sb-Be)
- Accelerator sources (D-D, D-T reactions)

Properties of neutron sources for imaging purpose

Source type	***nuclear reactor***	***neutron generator***	***spallation source***	***radio isotope***
Reaction	**fission**	**D-T fusion**	**spallation by protons**	**gamma-n-reaction**
used material	**U-235**	**deuterium, tritium**	**high mass nuclides**	**Sb, Be**
gain: primary neutron intensity [1/s]	**1.00E+16**	**4.00E+11**	**1.00E+15**	**1.00E+08**
beam intensity[cm-2 s-1]	**10^6 to 10^9**	**10^5**	**10^6 to n*10^7**	**10^3**
neutron energy	**fast, thermal and cold**	**fast, thermal**	**fast, thermal and cold**	**24 keV, thermal**
limitation of use	**burn up**	**life time tube**	**target life time**	**half life Sb-124**
typical operation cycle	**1 month**	**1000 h**	**1 year**	**0,5 year**
costs of the facility	**high**	**medium**	**very high**	**low**

Neutron energies

- high energy neutrons (E > 100 MeV)
- fast neutrons (from fission process): E ~ 1 MeV
- epithermal neutrons: E > 1eV
- thermal neutrons: E ~ 25 meV
- cold neutrons: E ~ 4 meV
- ultra-cold neutrons: E ~ 100 neV

➢ 15 orders of magnitude in energy

Neutron energies

- high energy neutrons (E > 100 MeV)
- fast neutrons (from fission process): E ~ 1 MeV
- epithermal neutrons: E > 1eV
- **thermal neutrons: E ~ 25 meV**
- **cold neutrons: E ~ 4 meV**
- ultra-cold neutrons: E ~ 100 neV

➢ 15 orders of magnitude in energy

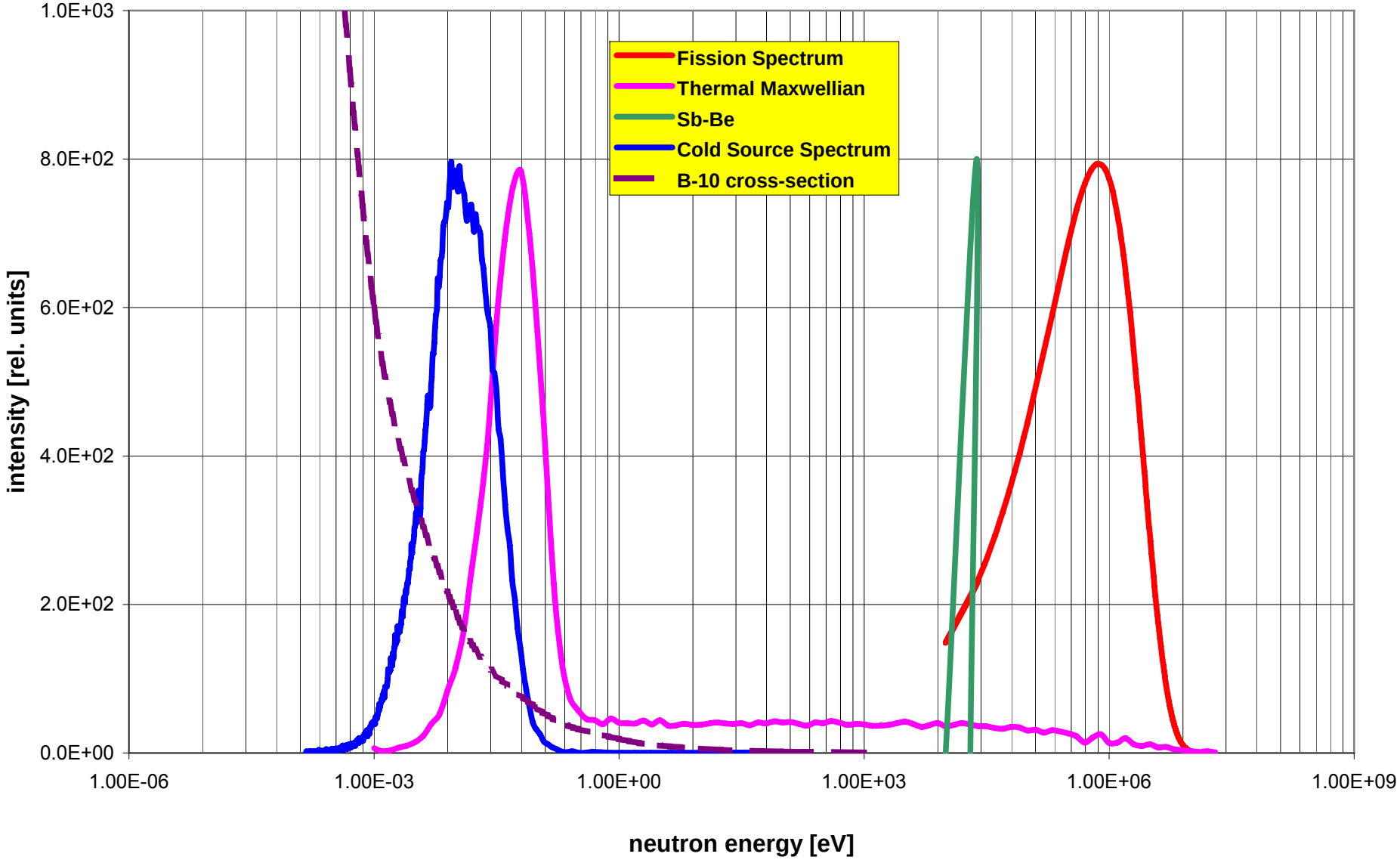
Fission Spectrum
Thermal Maxwellian
Sb-Be
Cold Source Spectrum
B-10 cross-section
1.0E+03
8.0E+02
6.0E+02
4.0E+02
2.0E+02
0.0E+00
intensity [rel. units]
1.00E-06
1.00E-03
1.00E+00
1.00E+03
1.00E+06
1.00E+09
neutron energy [eV]

Collimation

- to generate a quasi-parallel, clean beam
- by ***selection*** of suited neutrons
- collimation ratio: **L**(collator length)/**D**(aperture diameter) – typically several 100
- by ***filtering*** (against gamma radiation, against neutrons of different energies)
- to limit the radiation level at the detector position

The Neutron Radiography Station NEUTRA for thermal neutrons

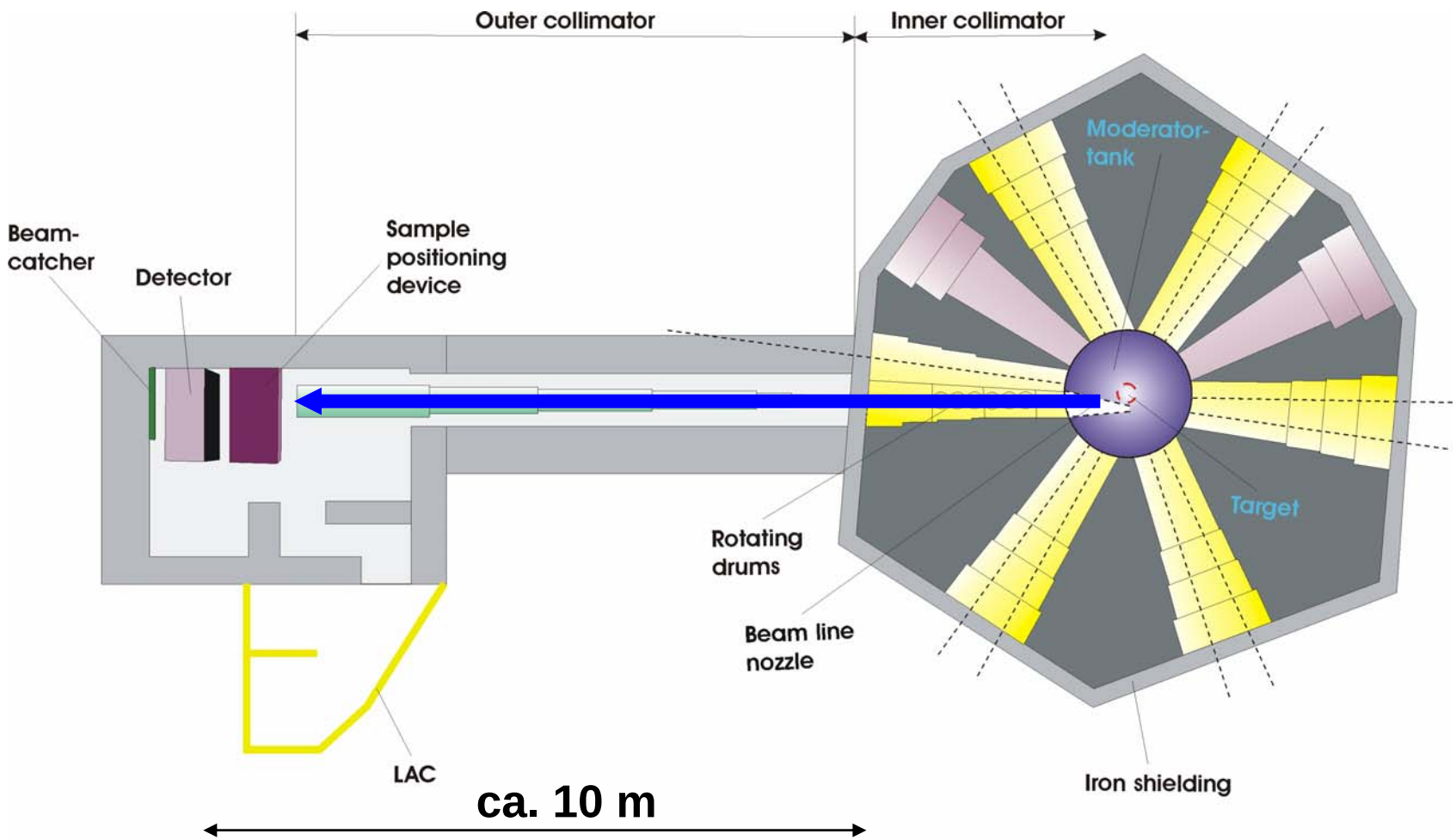

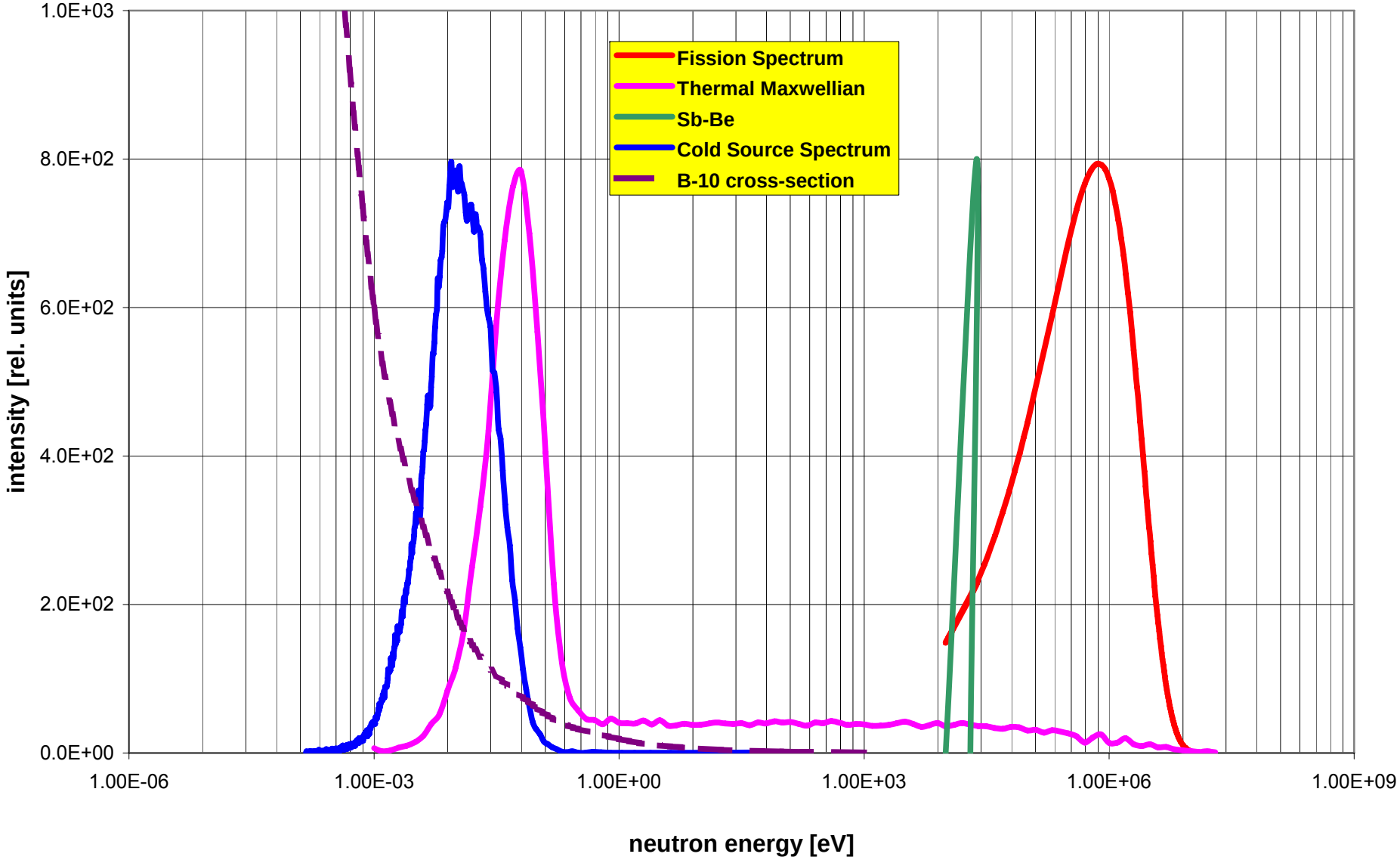
Fission Spectrum
Thermal Maxwellian
Sb-Be
Cold Source Spectrum
B-10 cross-section
1.0E+03
8.0E+02
6.0E+02
4.0E+02
2.0E+02
0.0E+00
intensity [rel. units]
1.00E-06
1.00E-03
1.00E+00
1.00E+03
1.00E+06
1.00E+09
neutron energy [eV]

The Neutron Radiography Station ICON for cold neutrons

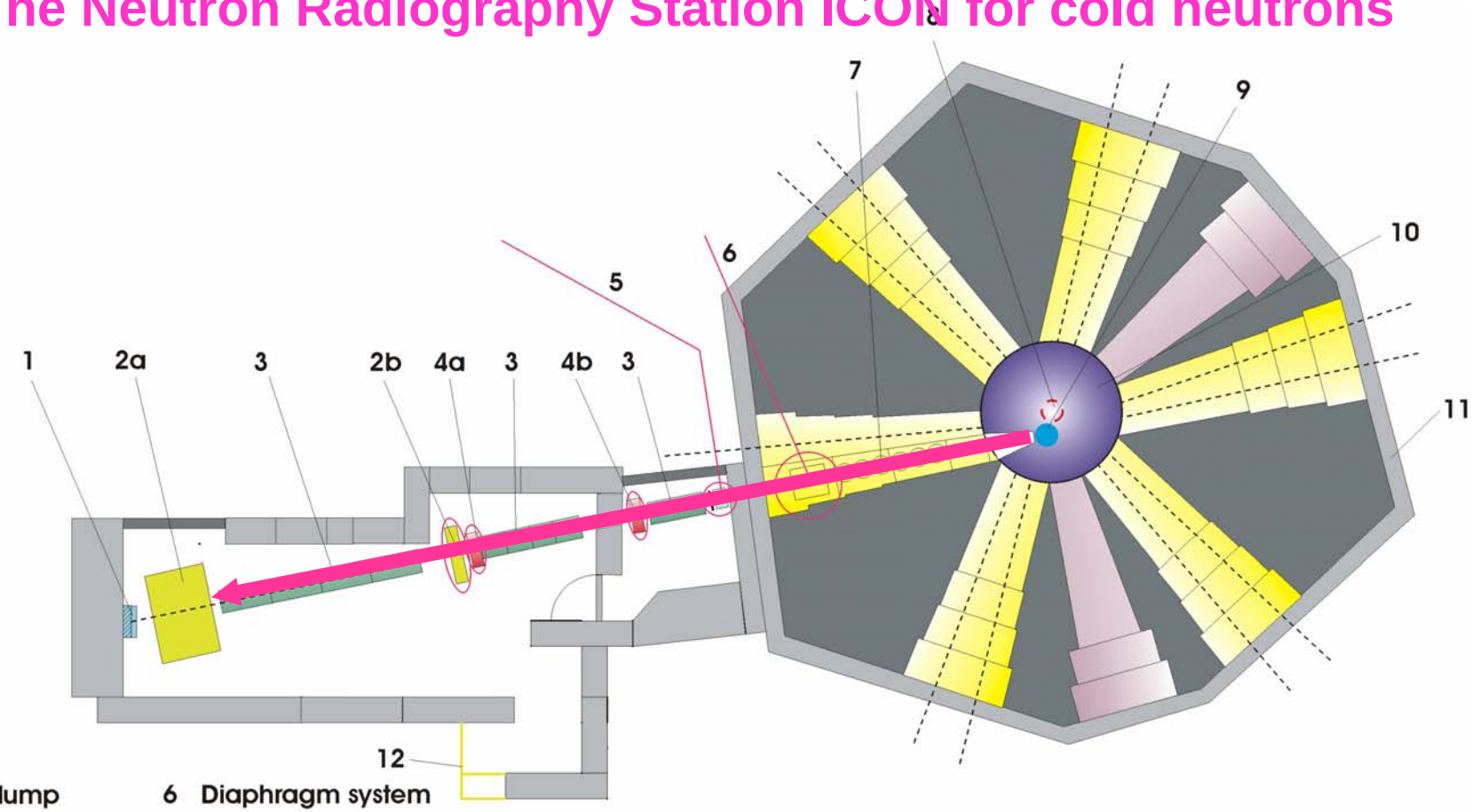

1 Beamdump
2a Sample position 1
2b Sample position 2
3 Flight tubes
4a Beam limiter
4b Beam limiter
5 Shutter
6 Diaphragm system
7 Rotating drums
8 Spallation target
9 Cold source (D_2)
10 Moderator tank (D_2O)
11 Concrete and iron shielding
12 access control area

In use since May 2005

ICON beam line @ SINQ

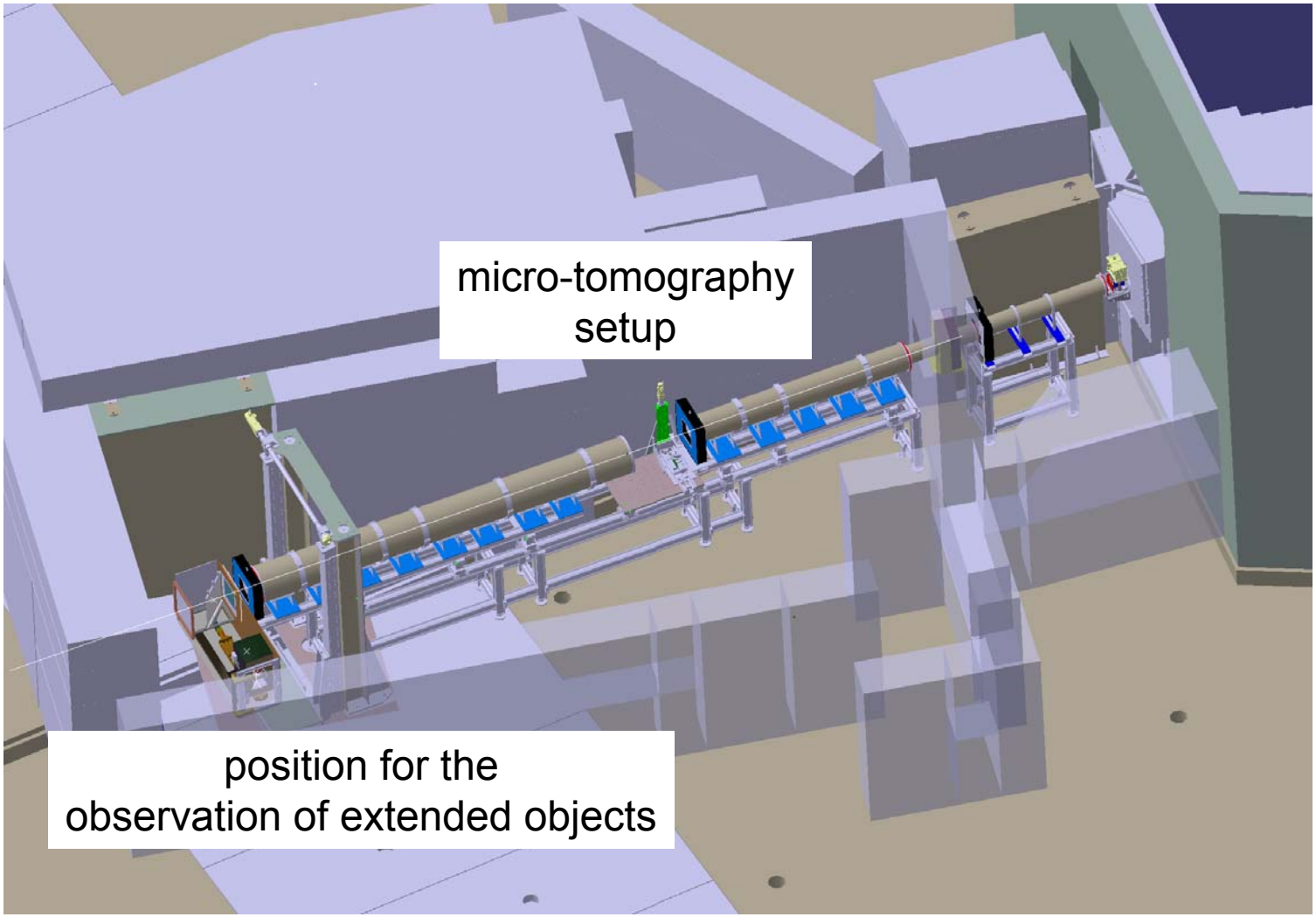

Properties of the neutron radiography stations at PSI

Facility	NEUTRA (operational since 1997)	ICON (under construction)
neutron flux density [cm^{-2} s^{-1}]	$3 \cdot 10^6$ - $2 \cdot 10^7$	> $5 \cdot 10^6$
collimation ratio L/D	250 – 550	Up to ~1000 dep. on the chosen aperture
beam size	∅ 15 – 40 cm	□ 8 – 30 cm dep. on the chosen aperture
spectrum	thermal	cold
mean energy [meV]	25	3

neutron detection for imaging

- no direct neutron detection possible

- a secondary nuclear process is needed
  (capture, fission, collision)

- main ***neutron imaging processes*** are using:

➢ scintillation
➢ photo-luminiscence by secondary particles + β, γ
➢ nuclear track detection
➢ chemical excitation
➢ collection of charge in semiconductors from Gd conversion

Capture reactions for thermal neutrons

$^{3}He + {}^{1}n \Rightarrow {}^{3}He + {}^{1}p + 0.77$ MeV

$^{6}Li + {}^{1}n \Rightarrow {}^{3}H + {}^{4}He + 4.79$ MeV

$^{10}B + {}^{1}n \Rightarrow {}^{7}Li + {}^{4}He + 2.78$ MeV (7%)

$\Rightarrow {}^{7}Li^{*} + {}^{4}He + 2.30$ MeV (93%)

$^{155}Gd + {}^{1}n \Rightarrow {}^{156}Gd + \gamma$´s + CE´s (7.9 MeV)

$^{157}Gd + {}^{1}n \Rightarrow {}^{158}Gd + \gamma$´s + CE´s (8.5 MeV)

^{235}U, ^{239}Pu $^{1}n \Rightarrow$ fission products + 80 MeV

Properties of neutron detection materials

reaction	σ_n [barn]	particle energy [MeV]	natural content	enrichment	price [US$ 2000]
$^{3}He(n,p)$	5333	p: 0.57 ^{3}H: 0.2	0.00014%		90 dm^{-3}
$^{6}Li(n,\alpha)$	940	α: 2.05 ^{3}H: 2.74	7.5%	95%	1.5 g^{-1} ^{6}Li Metall
$^{10}B(n,\alpha)$	3837	α: 1.47 ^{7}Li: 0.83	19.8%	99%	12 g^{-1} $^{10}B_2O_3$
$^{155}Gd(n,\gamma)$	60900	CE,s: 0.039 - 0.25	14.8%		
$^{157}Gd(n,\gamma)$	254000	CE´s: 0.029 - 0.23	15.7%	86%	8000 g^{-1} Gd_2O_3
$^{nat}Gd(n,\gamma)$	48890		100%		1.5 g^{-1} Gd_2O_3
$^{235}U(n,f)$	583	80 total	0.72%		
$^{239}Pu(n,f)$	748	80 total	0		

Detectors for digital imaging with neutrons

detector system	x-ray film and transmission light scanner	scintillator + CCD-camera	imaging plates	amorph silicon flat panel
max. spatial resolution [μm]	20 - 50	100 - 500	25 - 100	127 - 750
typical exposure time for suitable image	5 min	10 s	20 s	10s
detector area (typical)	18 cm x 24 cm	25 cm x 25 cm	20 cm x 40 cm	30 cm x 40 cm
number of pixels per line	4000	1000	6000	1750
dynamic range	10^2 (non-linear)	10^5 (linear)	10^5 (linear)	10^3 (non-linear)
digital format	8 bit	16 bit	16 bit	12 bit

Neutron detectors for imaging

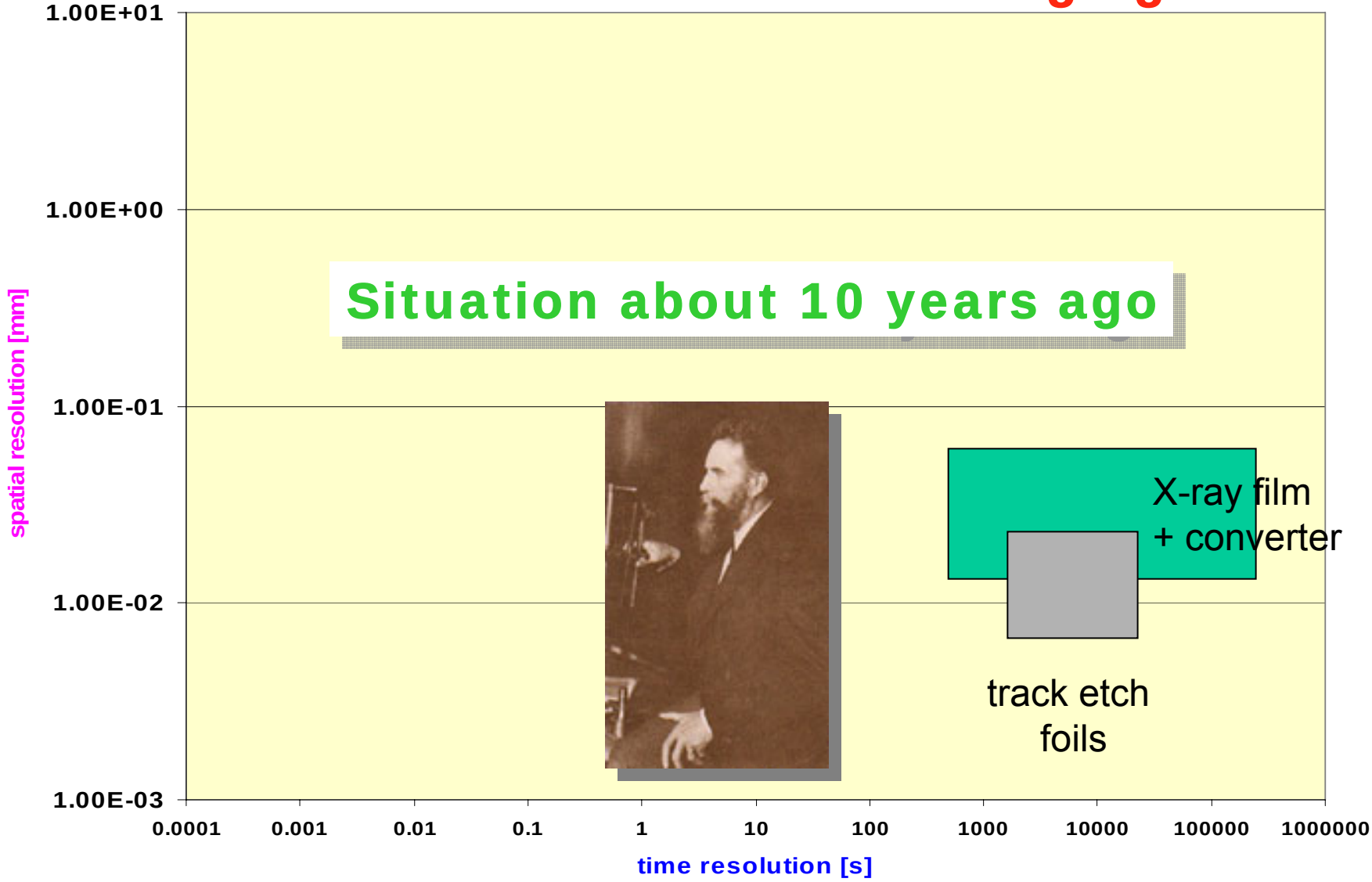

Neutron detectors for imaging

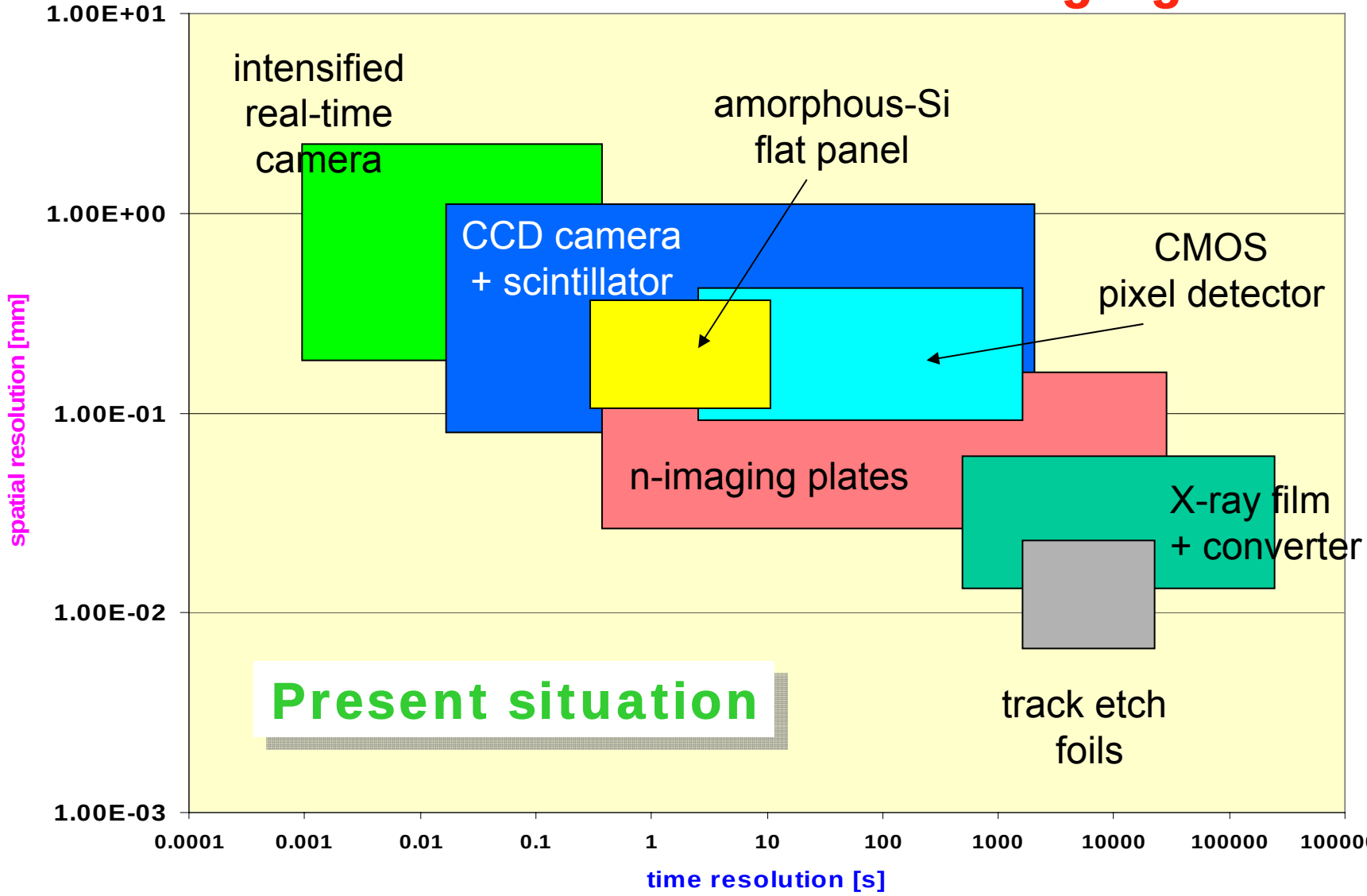

Neutron detectors for imaging

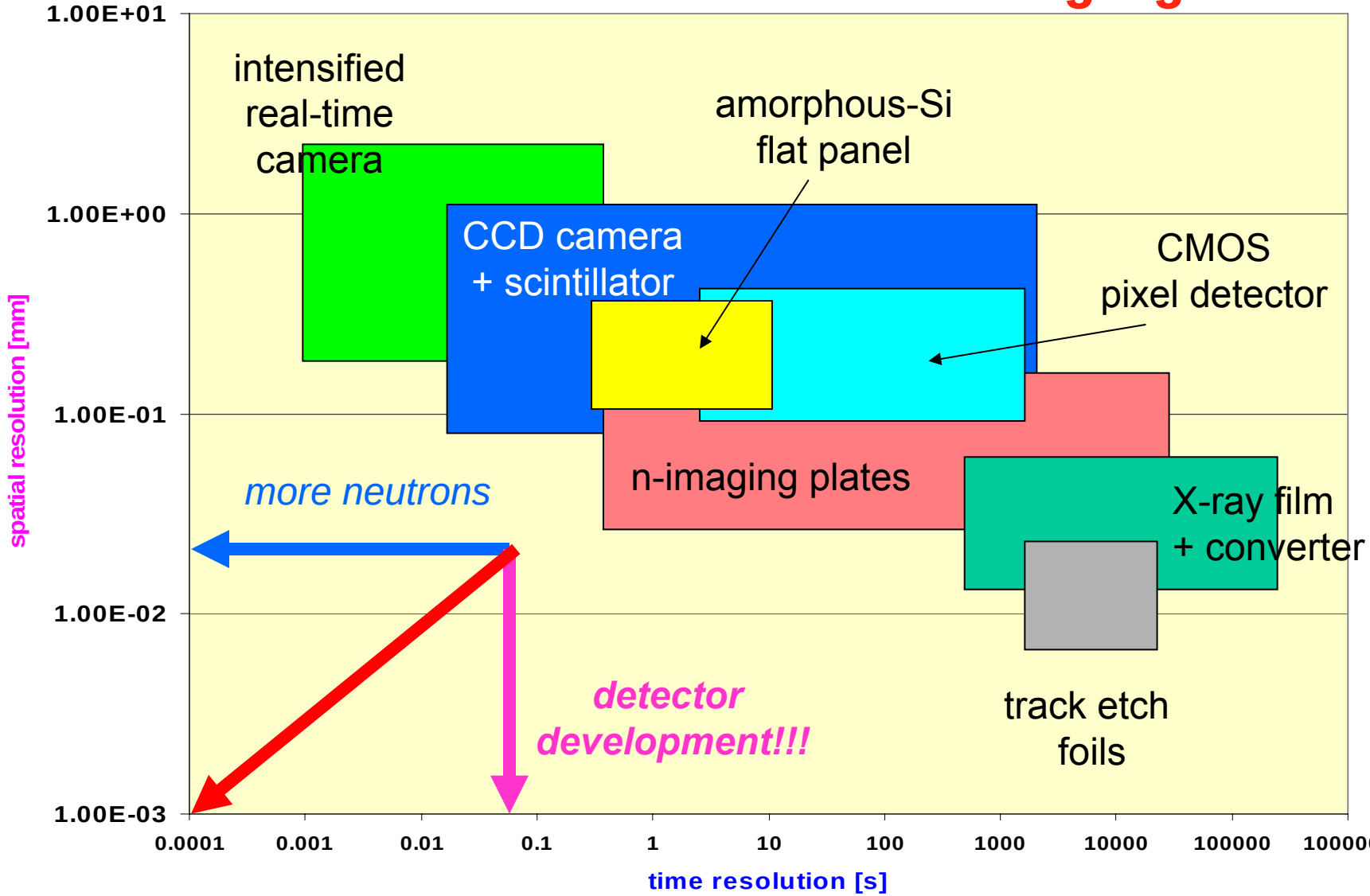

CCD-camera

- neutrons are hitting the scintillator and the emitted light will be detected by the high sensitive camera.

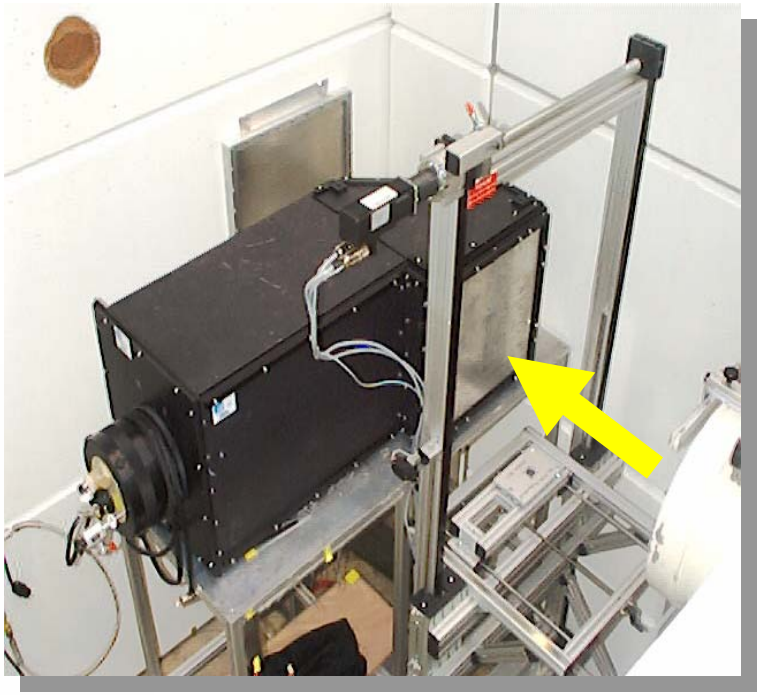

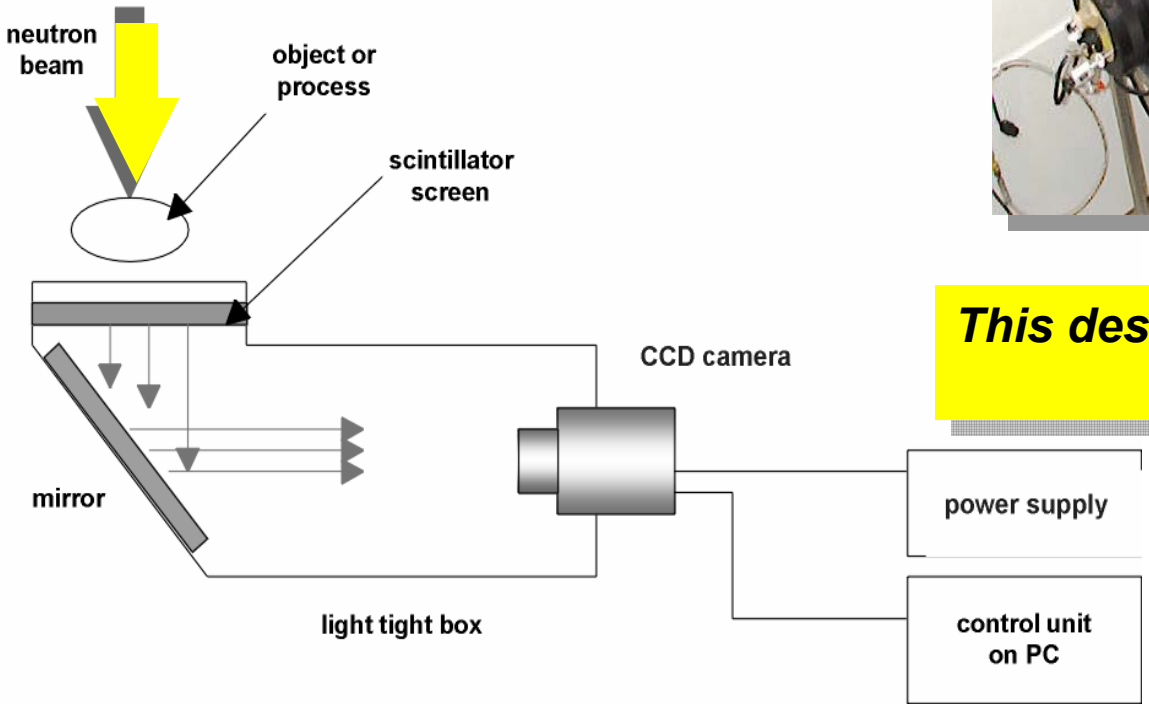

This design has become a common one is many labs

Neutron Imaging with a PILATUS -Module

Principle

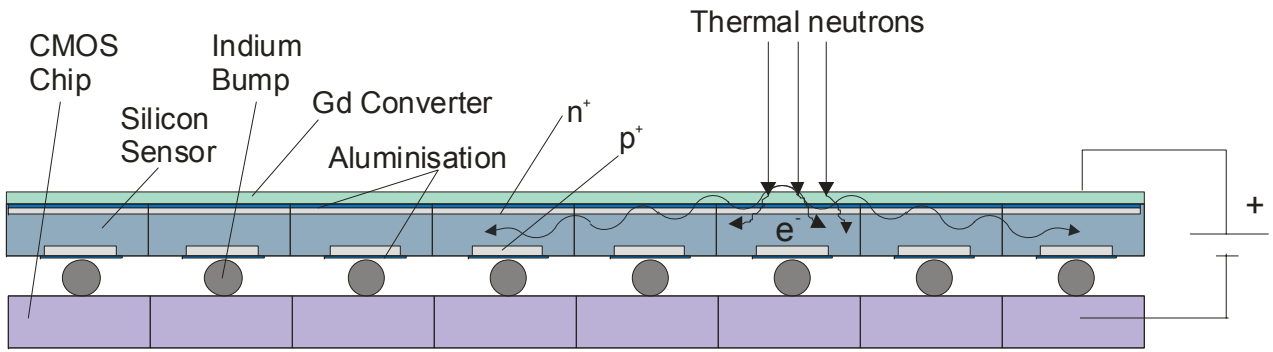

Pixel Electronics

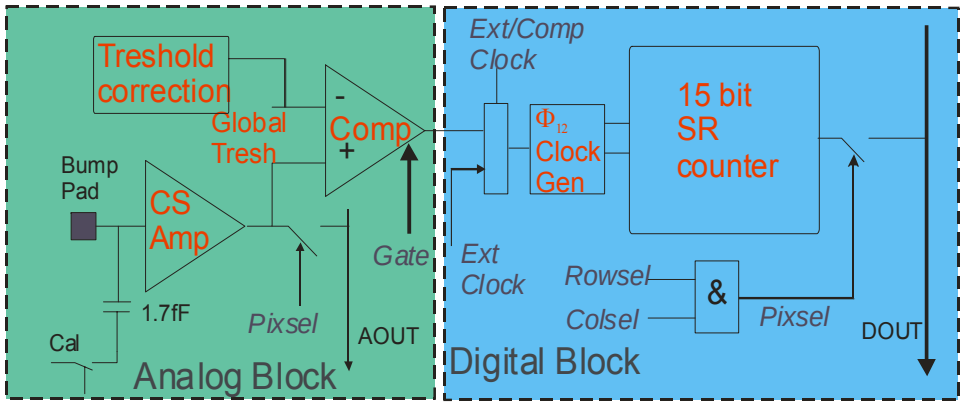

Features

- **No dark current**
- **No readout-noise**
- **Fast Gate: 100µs …secs**
- **Read-out time: 6.7ms**

active area: 3.5 cm * 8 cm

Foto of the array in a box

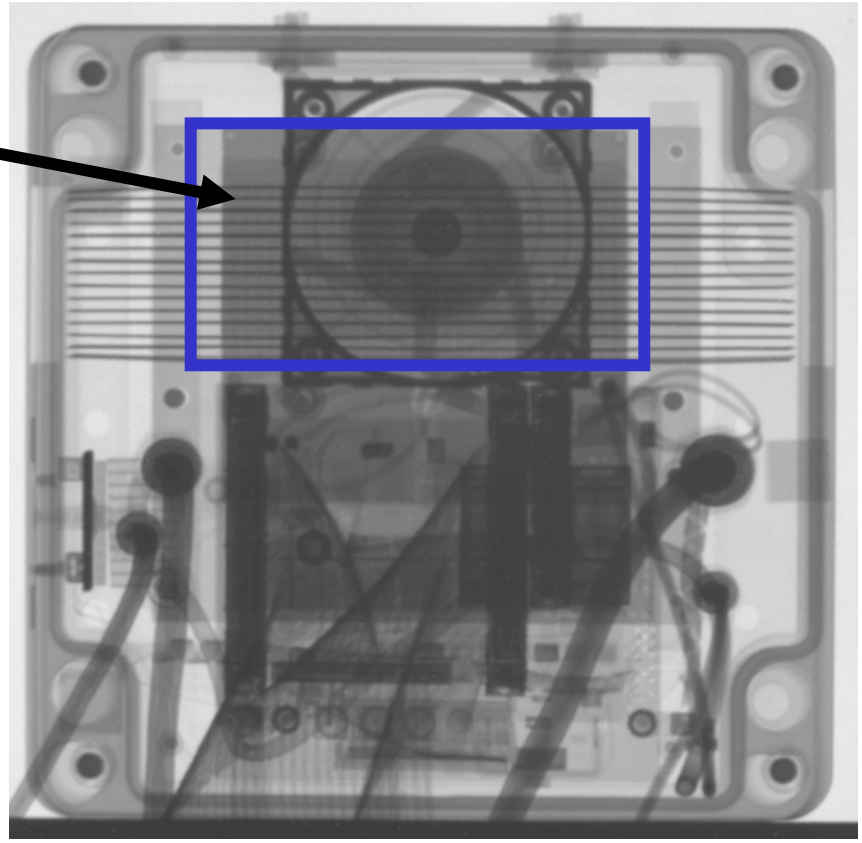

transmission image by neutrons

Comparison to Synchrotron Radiation Imaging

Detection lower limit: spatial resolution (*by the detector*)
Detection upper limit: object size (*beam size, transmission*)

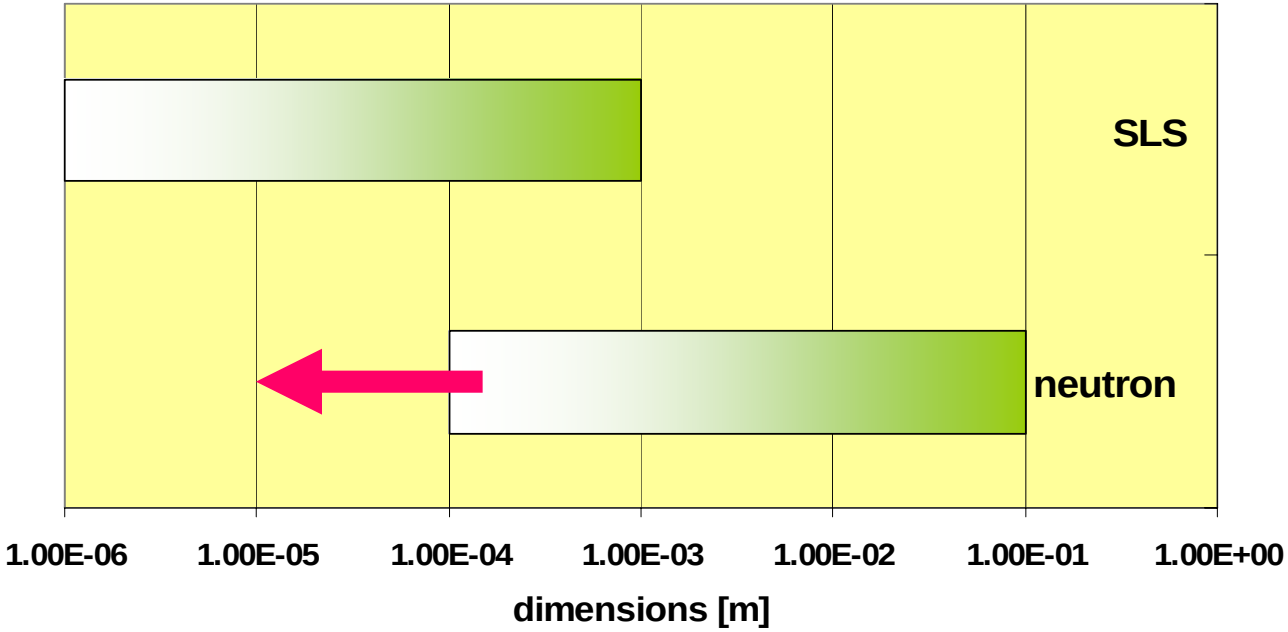

Different, but overlapping working area

Options for neutron imaging available at PSI

- Radiography with high spatial resolution
- Tomography on different size scale (4 cm to 40 cm)
- real-time imaging (up to 30 frames/sec. or triggered mode)
- Phase contrast neutron imaging
- Laminography
- X-ray enhanced neutron imaging
- *Later:* energy selective neutron imaging
- *Later:* micro-tomography with neutrons

The Principles of Neutron Tomography

B. Schillinger

1. Introduction

- A radiography picture is a **shadow image** of the investigated sample.

- Information about the internal distribution of the attenuation coefficient within the sample along beam direction is **lost in the single projection**.

- If the sample is rotated and **many different views** are taken, a tomographic reconstruction of that internal distribution can be performed.

- **Mathematical models** assume either a perfect parallel beam or a perfect point source.

- Neither case is exactly given for neutron tomography.

- It is therefore of great importance to shape the beam as to approximate ideal beam geometry best as possible.

Beam geometries for tomography

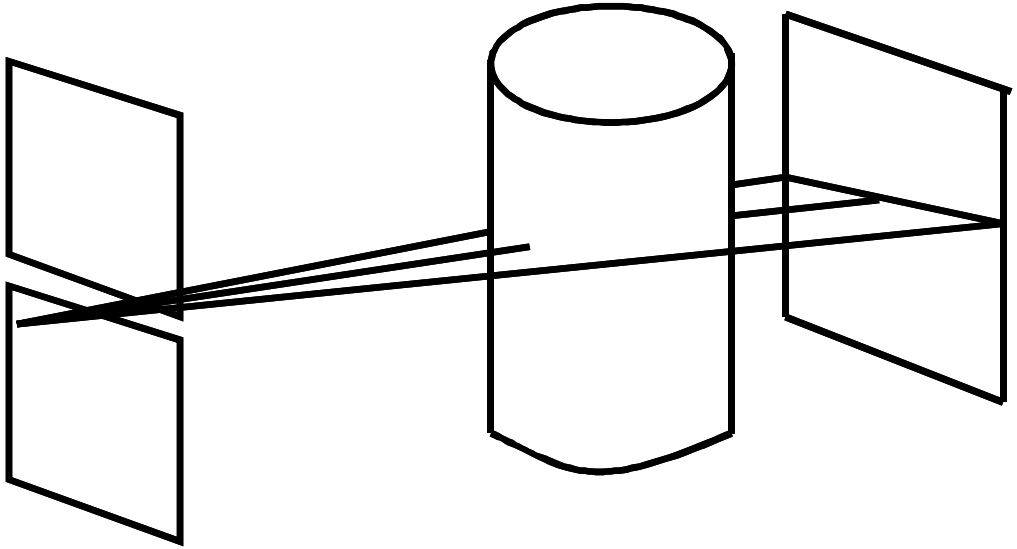

Fan beam geometry

This applies for a standard setup with an X-ray tube and a line detector.
The projection of the sample is magnified.
Reconstruction is done in an even plane.

Beam geometries for tomography

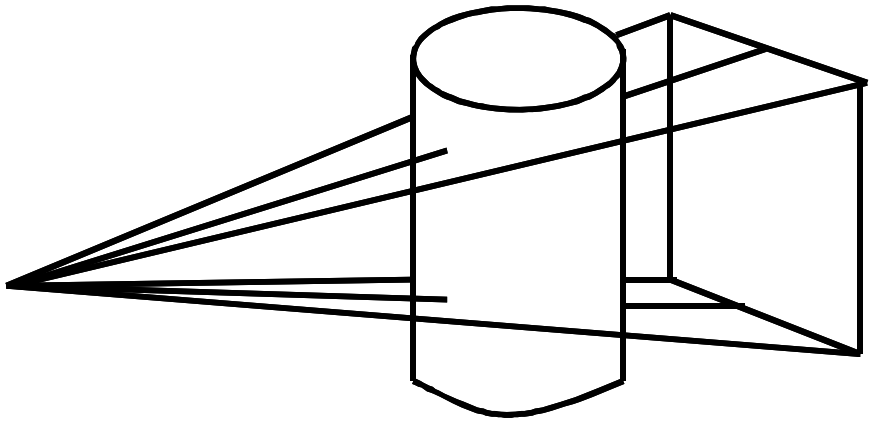

Cone beam geometry

Applies for a point source (LinAc, X-ray tube) and a two-dimensional detector.

The projection of the sample is magnified.

Reconstruction must be done in a 3D-Matrix.

Beam geometries for tomography

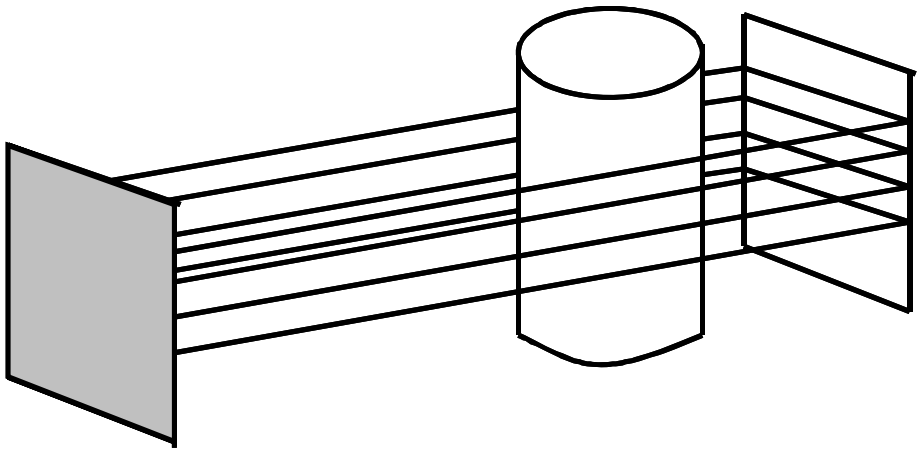

Parallel beam geometry

The simplest case - applies for a synchrotron light source and a line or 2D-detector.
There is no magnification.

For neutrons, none of the cases is really true,
we try to approximate parallel beam geometry as good as possible.

2. The tomography principle

2.1 Projection and Radon Transform

The following assumptions are made:

- the examined object is penetrated by a bundle of parallel rays. The procedure can be described in a plane (x,y).

- The beam is attenuated by the two-dimensional attenuation coefficient Σ(x,y).

- Scattered neutrons do not hit the detector, so scattering looks like absorption.

- The beam is mono-energetic.

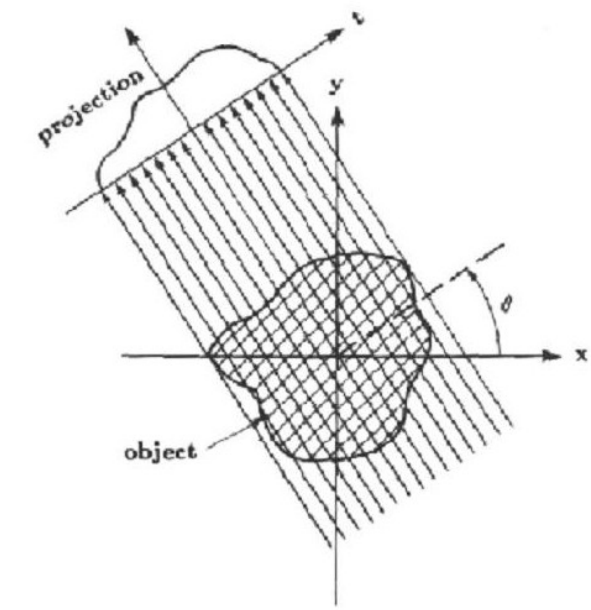

space domain

Each detector element is hit by a number of neutrons

$$N = N_0 \cdot e^{-\int_{beam\ path} \Sigma(x,y)\,ds}$$

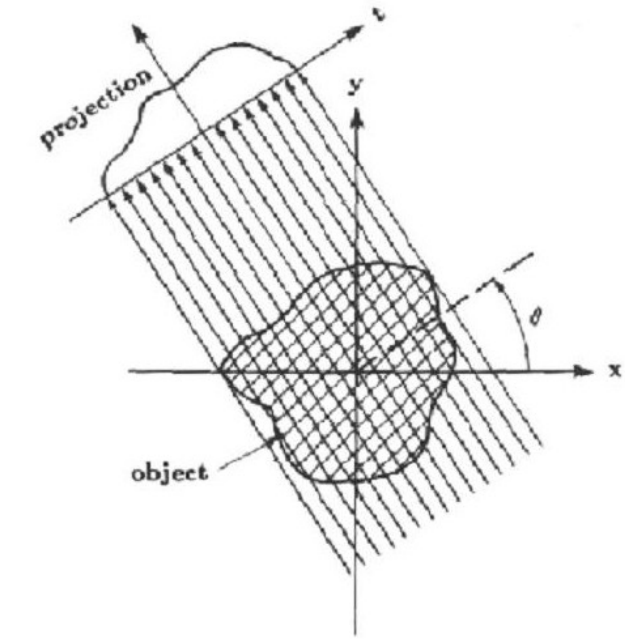

space domain

with N_0= number of incident neutrons
and the linear attenuation coefficient Σ(x,y) at position (x,y).

Integration is performed along the straight beam path s through the plane.

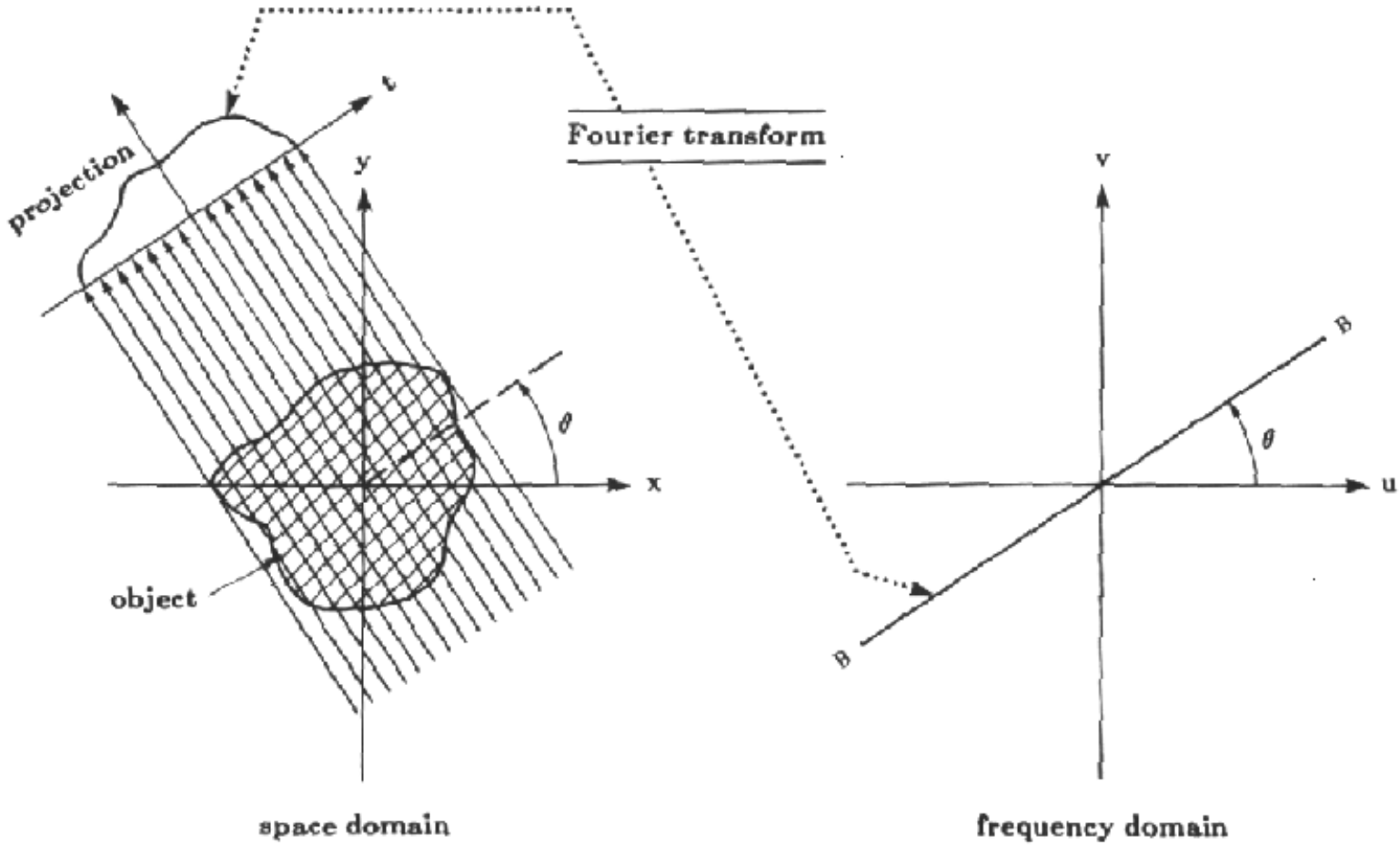

Projection $P_\theta(t)$ of a two-dimensional slice
and the position of its Fourier transform $P_\theta(\omega)$ in frequency domain.

We can give the projection of the two-dimensional slice as a one-dimensional function of the variable t perpendicular to the rays:

$$p_\theta(t) = \int_{ray(\theta,t)} \Sigma(x,y)ds$$

$$= \int_{-\infty}^{+\infty} \int_{-\infty}^{+\infty} \delta(x\cos\theta + y\sin\theta - t)\Sigma(x,y)dxdy$$

$$with \quad t = x\cos\theta + y\sin\theta$$

This is the ***Radon Transform .***

It can be derived from measurement as

$$p_\theta(t) = -\ln \frac{N_\theta(t)}{N_0(t)}$$

For parallel beam geometry, an angular range of 0 to 180° it is sufficient.

The integration causes the loss of the spatial information about the distribution of Σ(x,y) along the ray path.

But as each ray represents an independent measurement, the spatial information perpendicular to the ray direction (i.e. in direction θ,t) is still present.

2.2 The Fourier Slice Theorem

The one-dimensional Fourier-Transform of the projection $P_\theta(\omega)$ is

$$P_\theta(\omega) = \int_{-\infty}^{+\infty} p_\theta(t) e^{-2\pi i \omega t} dt$$

and the two-dimensional Fourier-Transform S(u,v) of the slice to be reconstructed is:

$$S(u,v) = \int_{-\infty}^{+\infty} \int_{-\infty}^{+\infty} \Sigma(x,y) e^{-2\pi i (ux+vy)} dxdy$$

These combined deliver the Fourier Slice Theorem:

$$P_\theta(\omega) = S\ (\omega\cos\theta, \omega\sin\theta) \equiv S\ (\omega, \theta)$$

Which can be worded as:

"The one-dimensional Fourier Transform $P_\theta(\omega)$ of a parallel projection of a distribution μ(x,y), taken under an angle θ, is identical with a single line within the two-dimensional Fourier Transform S(u,v) of the distribution Σ(x,y) that encloses the angle θ with the u-axis."

For reminder, again the representation in the spatial and in the Fourier Domain:

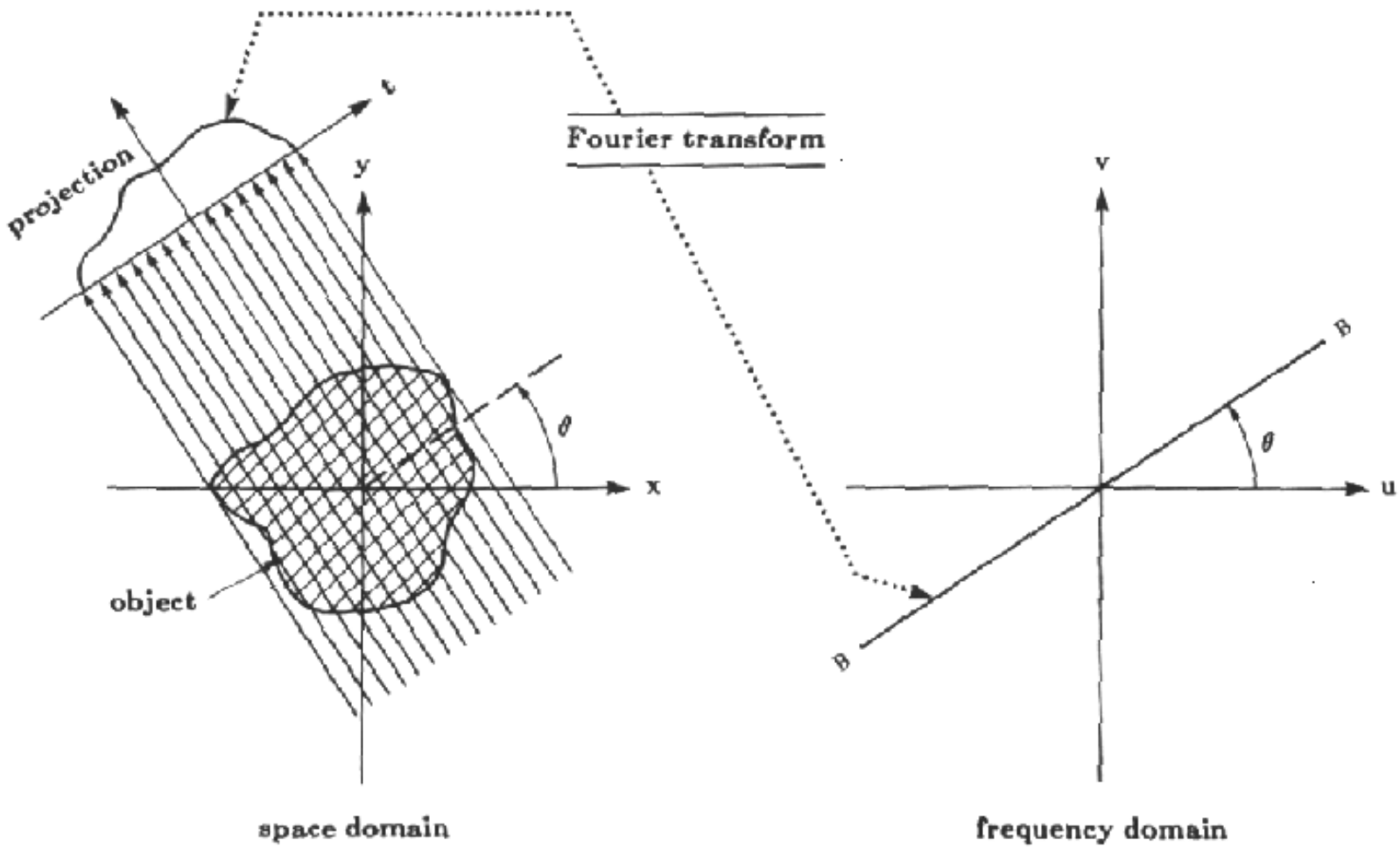

In theory, it would be possible to fill the entire Fourier space by measuring an infinite number of projections and then to obtain the distribution $\mu(x,y)$ by a two-dimensional Fourier back-transform of S(u,v):

$$\Sigma(x,y) = \int_{-\infty}^{+\infty} \int_{-\infty}^{+\infty} S(u,v) e^{2\pi i(ux+vy)} du\, dv$$

2.3 *Filtered Back-projection*

In reality, the number of rays and the number of projections is limited. The function S(u,v) is known only at a few points on radial lines.

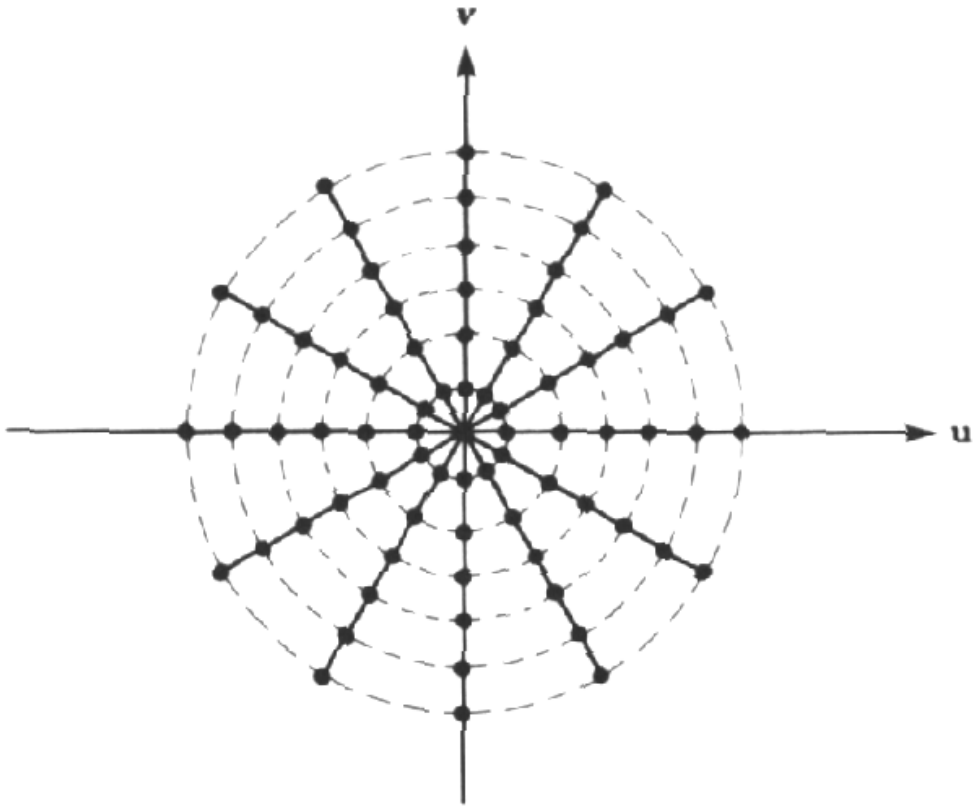

Measured values in frequency domain

•These points must be **interpolated** to a quadratic mesh.

•With increasing radial distance, the density of measured values decreases, and interpolation **incertainty increases**.

•A simple reconstruction can be performed by simply **summing up the two-dimensional Fourier Transforms** of the single lines.

•Because of the linearity of the Fourier Transform, this can be done either in spatial or in frequency domain.

•But as the density of measured values decreases towards **high frequencies**, the high frequencies do not get enough weight, and the reconstructed image appears smoothed or smeared.

Each of k projections over 180° must deliver the information for a "cake slice" of width $2\pi|\omega|/k$.

But as it delivers only a single line, it is weighted with a ramp filter of height $2\pi|\omega|/k$, so that the new wedge has the same "mass" as the cake slice.

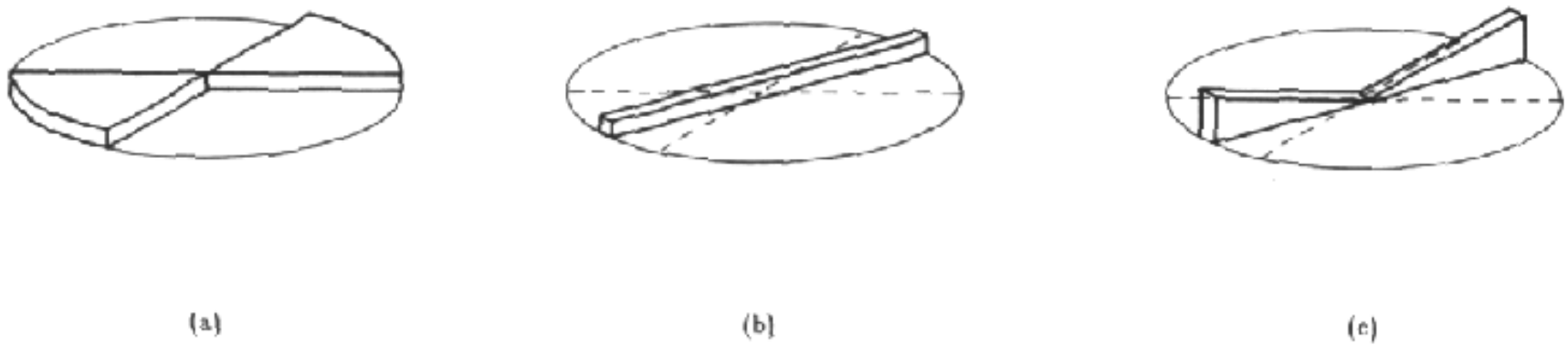

required, real and filtered representation of the data in frequency domain

The filter |ω| can be obtained mathematically exact by transformation to polar coordinates in frequency space. Then we obtain

$$\Sigma(x,y) = \int_0^{\pi} \int_0^{+\infty} S(\omega,\theta) e^{2\pi i \omega (x\cos\theta + y\sin\theta)} |\omega| \, d\omega \, d\theta$$

$$= \int_0^{\pi} \int_0^{+\infty} S(\omega,\theta) e^{2\pi i \omega t} |\omega| \, d\omega \, d\theta \qquad with \quad t = x\cos\theta + y\sin\theta$$

If we now substitute the one-dimensional Fourier Transform $P_\theta(\omega)$ of the projection at angle θ for the two-dimensional Fourier Transform $S(\omega,\theta)$, we obtain

$$\Sigma(x,y) = \int_0^{\pi} \left[\int_0^{+\infty} P_\theta(\omega) e^{2\pi i \omega t} |\omega| \, d\omega \right] d\theta \qquad with \quad t = x\cos\theta + y\sin\theta$$

$$= \int_0^{\pi} Q_\theta(x\cos\theta + y\sin\theta) \, d\theta \qquad with \quad Q_\theta(t) = \int_0^{+\infty} P_\theta(\omega) e^{2\pi i \omega t} |\omega| \, d\omega$$

This Equation describes a filter operation with the filter |ω|.

$Q_\theta(t)$ is called **"filtered projection".**

These filtered projections are "back-projected" onto the reconstruction field:
Each filtered projections $Q_\theta(t)$ contributes the same value to all points of the reconstruction field along the original ray.
The filtered back-projection is being "smeared" along the original ray path across the reconstruction field.

The filtered back-projection is being "smeared" along the original ray path across the reconstruction field.

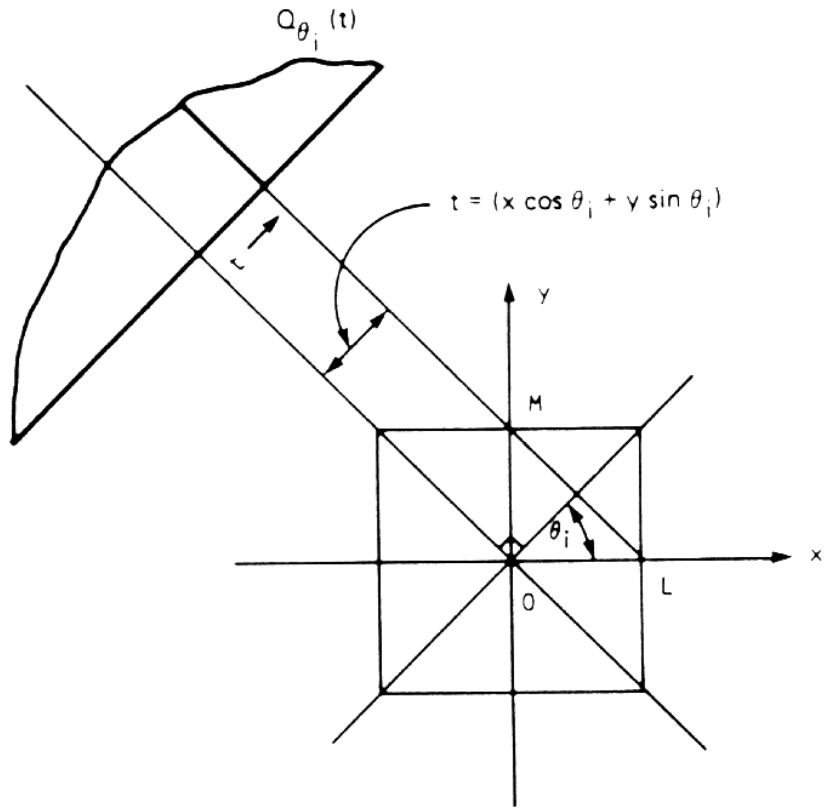

Back-projection of filtered data

The maximum spatial frequency is given by Nyquists theorem by the distance T between two detector elements as

$$\omega_{\max} = 2\pi \cdot \frac{1}{2T}$$

The simple multiplication of $P_\theta(\omega)$ by ω in the frequency domain can be replaced by a convolution of $p_\theta(t)$ with the Fourier Transform of $|\omega|$ in the spatial domain:

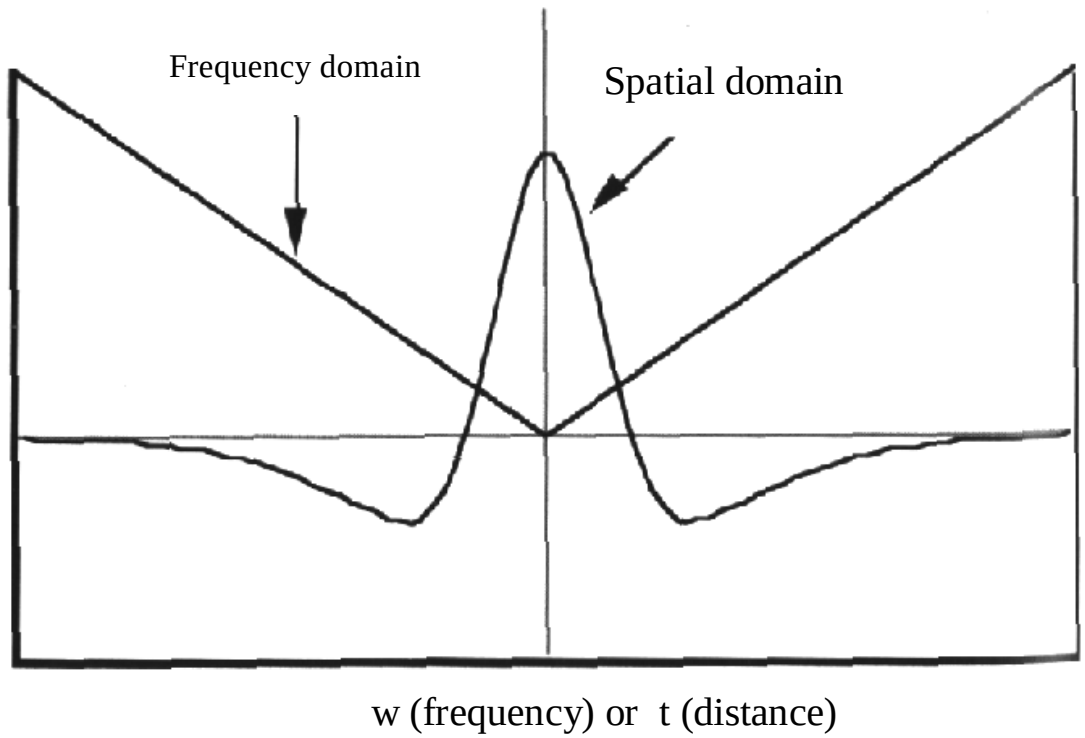

The ideal filter $|\omega|$ in spatial and frequency domain

•Difficulties with the ideal filter $|\omega|$ occur with noisy data, as noise consists mainly of high frequencies, which are much enhanced by this filter.
•The ideal filter is therefore often replaced by **special filter functions that decrease again towards high frequencies.**
•For neutrons, the inherent beam unsharpness (see below) often attenuates most high frequencies towards the Nyquist limit.

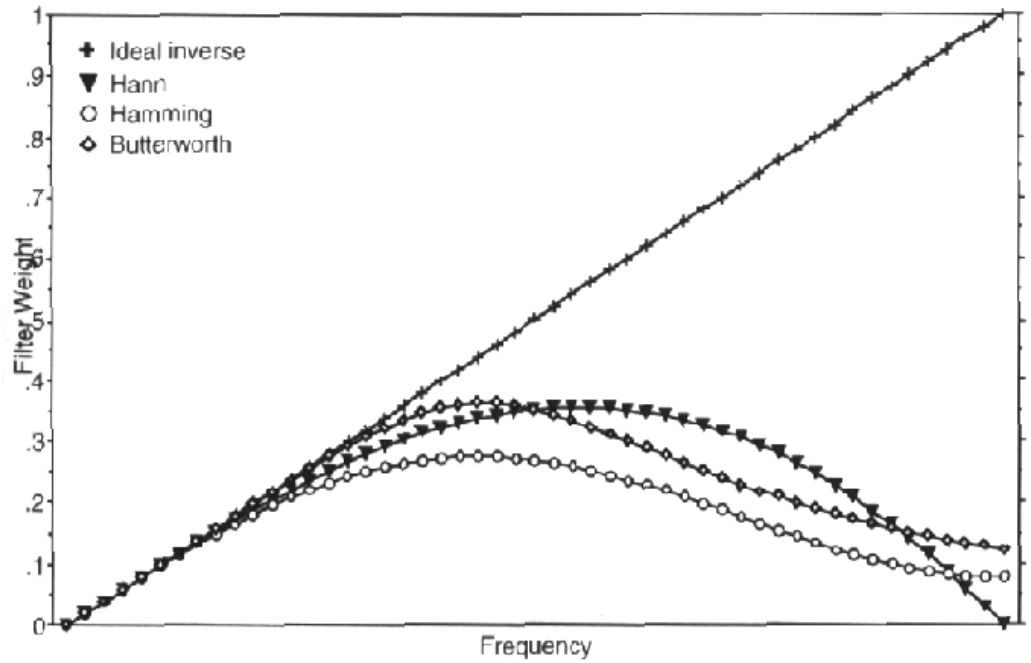

The ideal filter $|\omega|$ and some alternative functions

2.4 Number of projections

The number of projections should be in the same order as the number of rays in one projection.
For M projections with N rays over 180° , the angular increment δ between two consecutive projections is given in Fourier space as

$$\delta = \frac{\pi}{M}$$

For distance T between two neighboring rays, the highest measured spatial frequency ω_{max} in the projection is given by Nyquist's Theorem as

$$\omega_{\max} = \frac{1}{2T}$$

This is the radius of a disk in the frequency domain that contains all measured values.
The distance d between two consecutive values on the circle is:

$$d = \omega_{\max} \cdot \delta = \frac{1}{2T}\frac{\pi}{M}$$

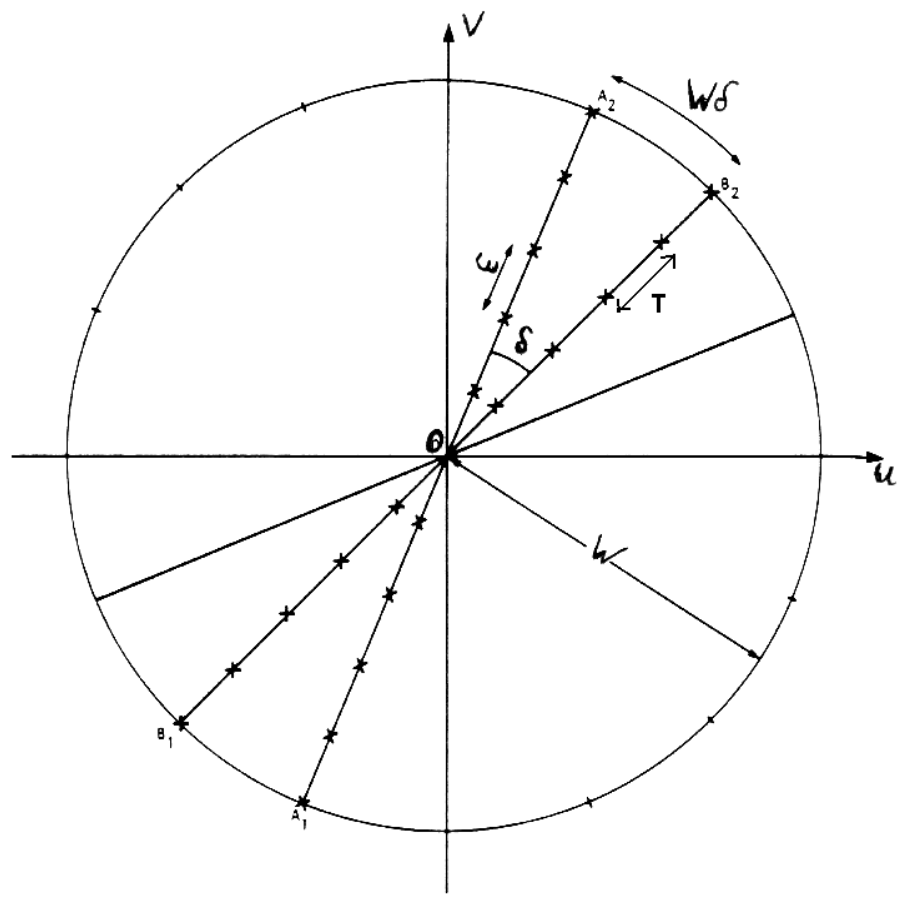

Density of measured values in frequency domain

For N measured values for each projection in spatial domain, there are also N measured values for each measured line in the frequency domain, so that the distance ε between two consecutive measured values on a radial line (or diameter) in frequency domain is given as

$$\varepsilon = \frac{2\omega_{\max}}{N} = \frac{1}{TN}$$

For the worst azimuthal resolution in frequency domain to match the radial resolution, we must demand:

$$\frac{1}{2T}\frac{\pi}{M} \approx \frac{1}{TN}$$

$$\frac{Number\ of\ \ projections}{Number\ of\ \ rays} = \frac{M}{N} \approx \frac{\pi}{2}$$

For **practical neutron radiography**, most detector systems cannot - at least for sub-millimeter resolution - measure down to the nominal Nyquist resolution given by their pixel size.

The greatest limiting factor is almost always the geometry of the neutron beam and its deviation from the ideal parallel ray model.

Present layout of the tomography setup at NEUTRA

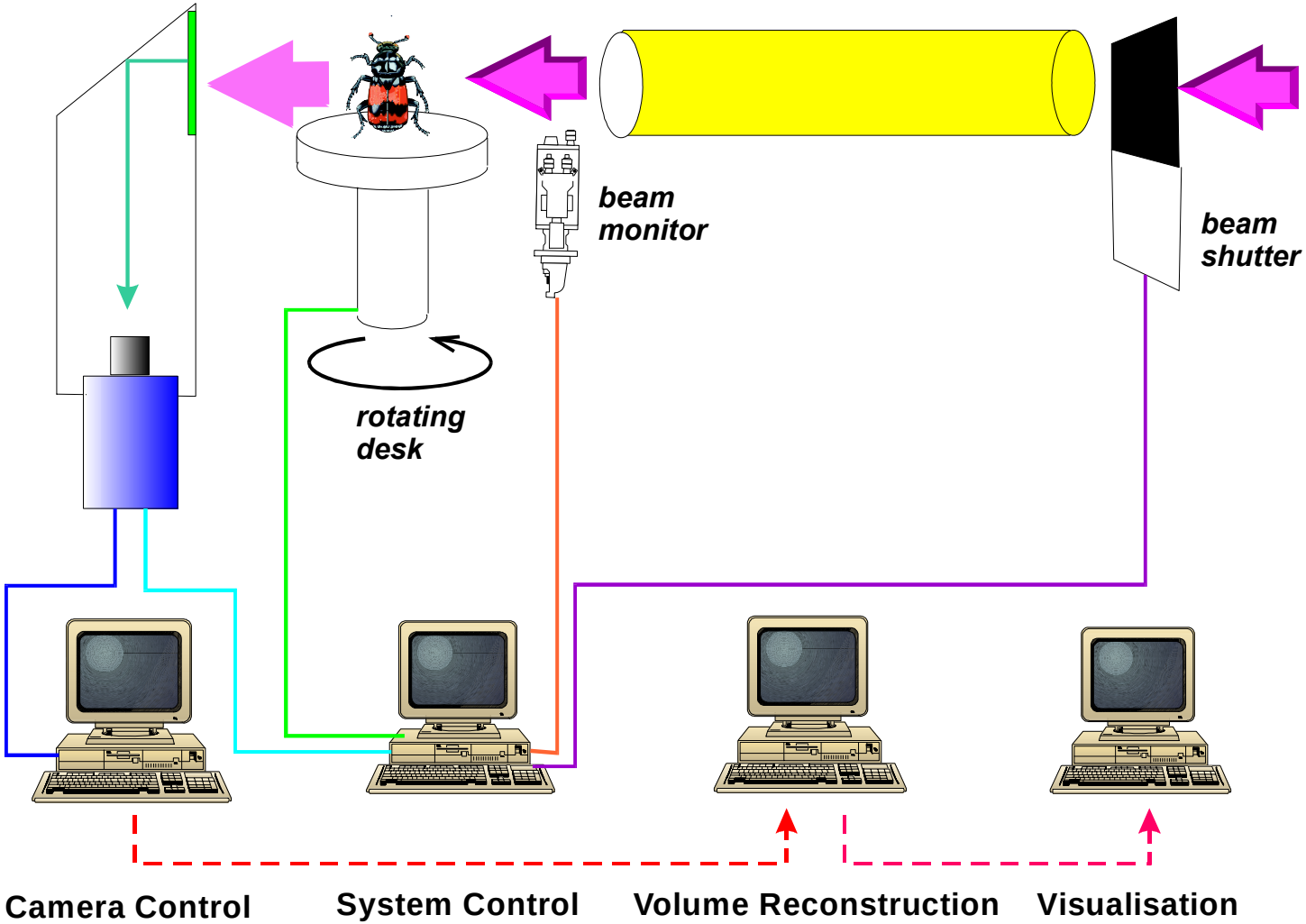

Sequence for the neutron tomography reconstruction

- Acquisition of N+1 projections of the object rotated in N steps over 180° around its vertical axis
- Spot filtering and normalization, determination of the centre of rotation
- Building of the sinogram = rearrangement of the projection values for one single slice
- Reconstruction according to the “Filtered back-projection” algorithm
- Results as a three-dimensional matrix of attenuation coefficients $\Sigma(x,y.z)$

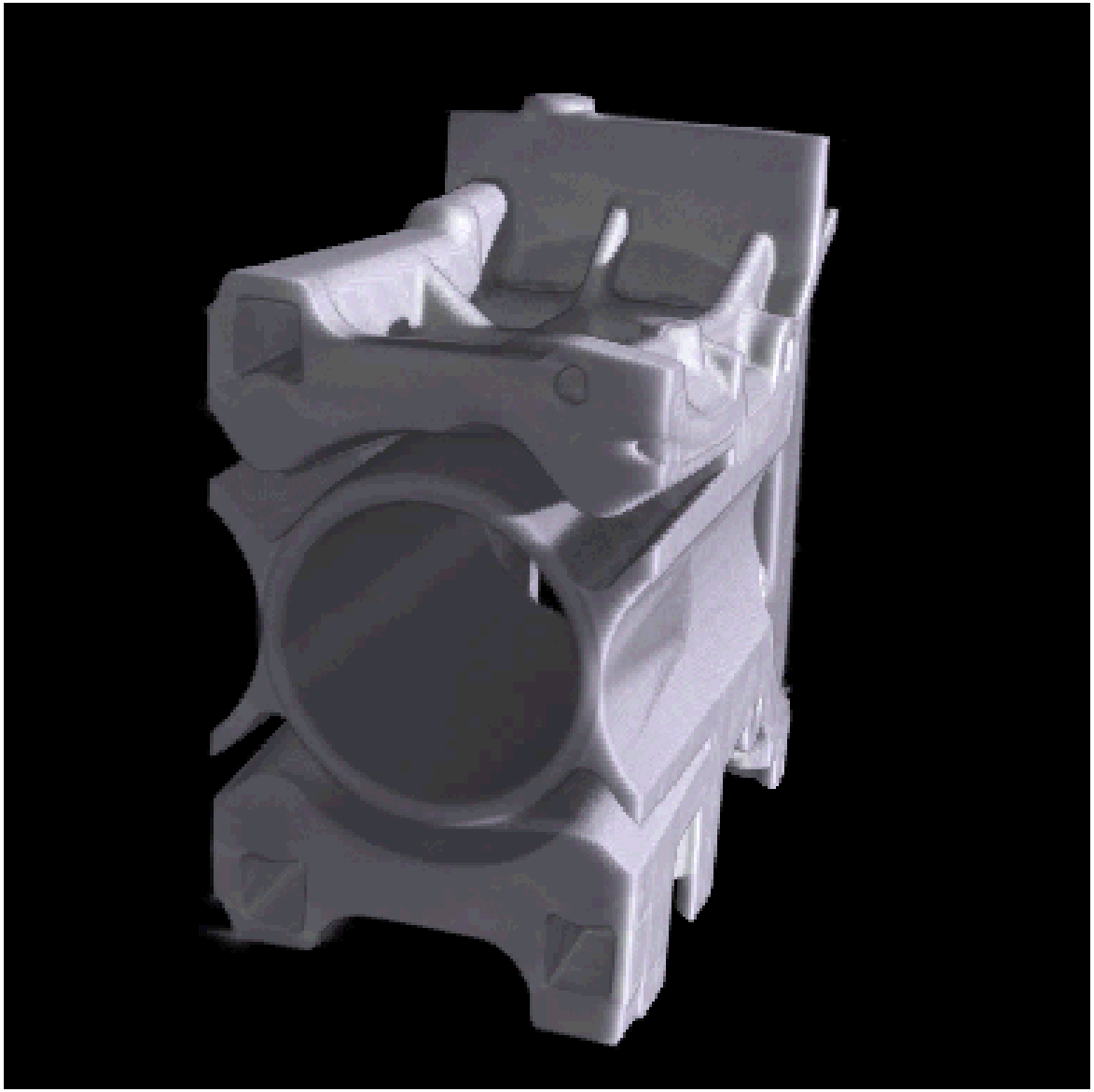

Non-invasive investigation of objects from cultural heritage

example:

bronze sculpture
"The Sun"
made by
Jaohan Gregor van der Schardt

height: 45.7 cm

tomography set produced in two separate runs-data unified

Johan Gregor van der Schardt (1530-after 1581),
cast by Georg Labenwolf (?-1585)

Sol (The Sun)

Nuremberg, c. 1570-1581

Height 45.7 cm

Rijksmuseum, Amsterdam

Inv. no. BK-1977-24

PROJECT COORDINATION

Robert van Langh
Dick Visser

SPECIAL THANKS TO

Eberhard Lehmann
Peter Vontobel
Frits Scholten

animation by Mirko Estermann

Time dependent investigations with neutrons

- the opportunity to make time dependent investigations is limited by the ***beam intensity*** and the ***detector efficiency***
- In the case of repetitive processes, ***triggered options*** and superposition of frames can be exploited
- It is to optimise between image quality and time resolution

Piston movement
of a running motorcar
engine

obtained at 1000 rpm

Freude am Fahren

Yamaha motor

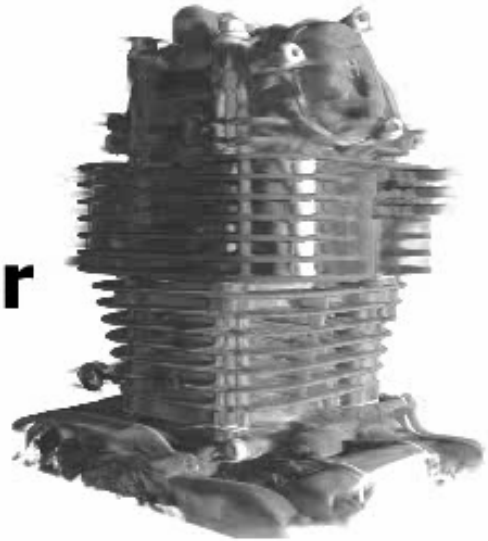

recorded at

NEUTRA NEUTRONENRADIOGRAPHIE @ PAUL SCHERRER INSTITUT PSI

Resin injection into a wooden sample:

Leaf 15 cm long

direct run

Resin injection into a wooden sample:

Leaf 15 cm long

referenced to original state

Energy selective NR investigations

- Using a turbine type selector
- Using a beam line on a pulsed neutron source with the TOF option
- To cut out parts of the spectrum by absorbers

Experiments at the Bragg edges of the materials

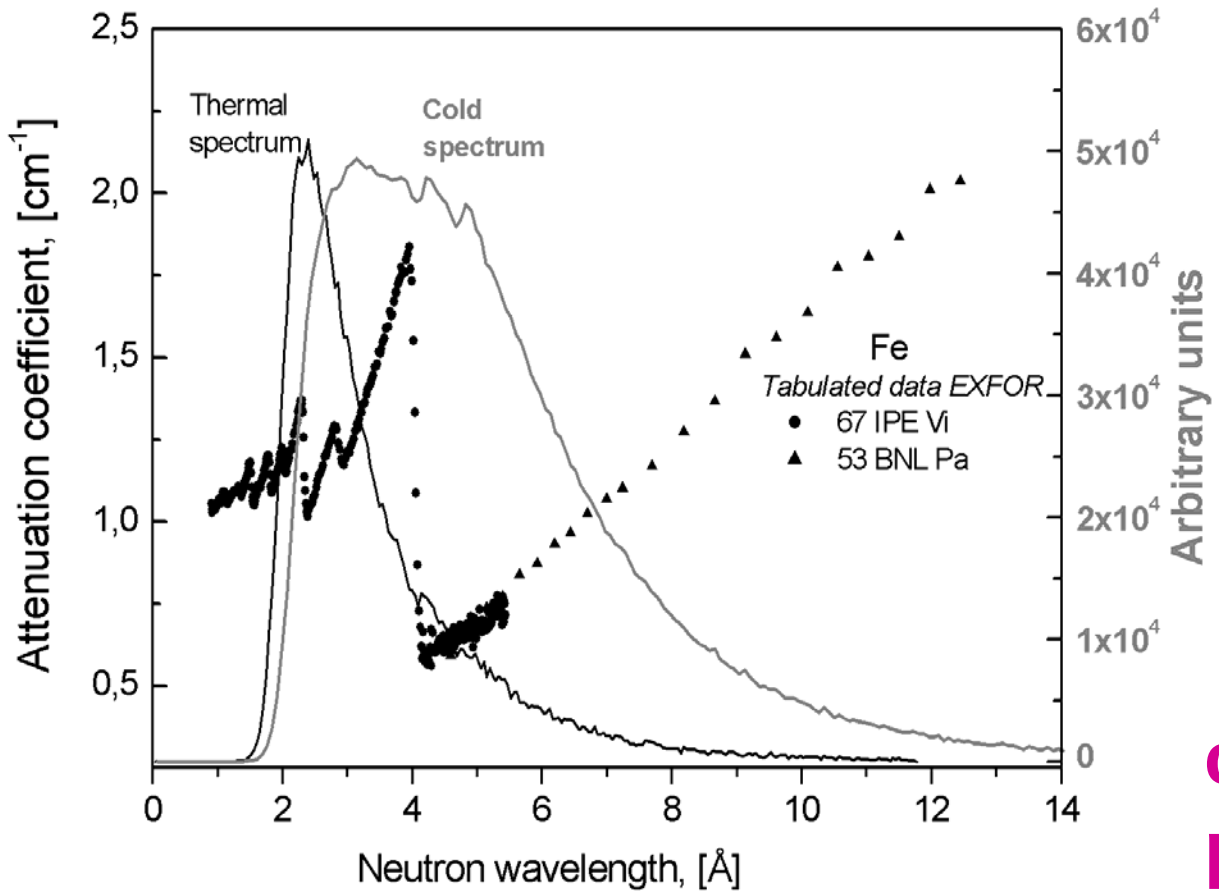

cold spectrum preferred !

Experiment 1:

neutron energy selector at the PGA neutron guide 15 of SINQ

work was done as collaboration between Uni Fribourg, PSI (CH) and TU Munich (D)

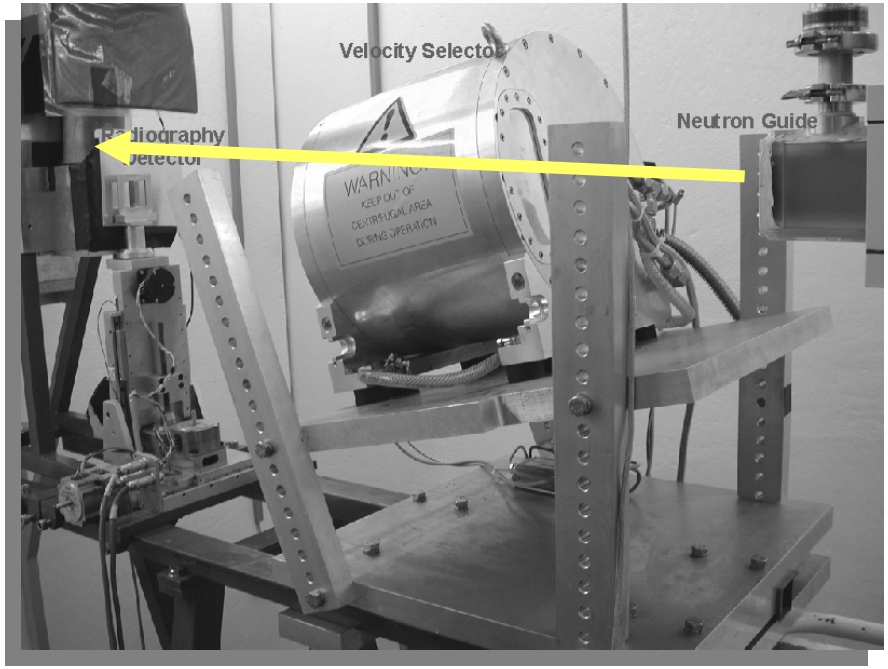

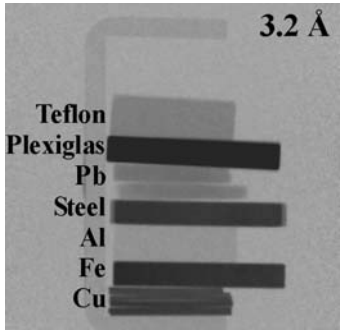

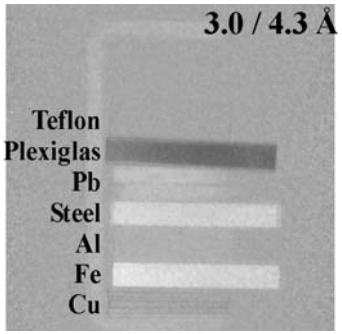

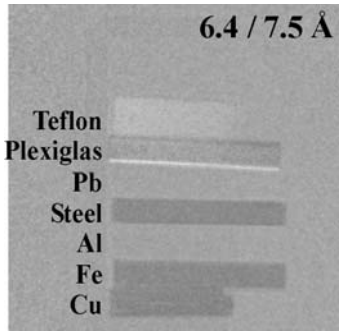

Application of referencing

Example: spark plug, N. Kardjilov (TUM)

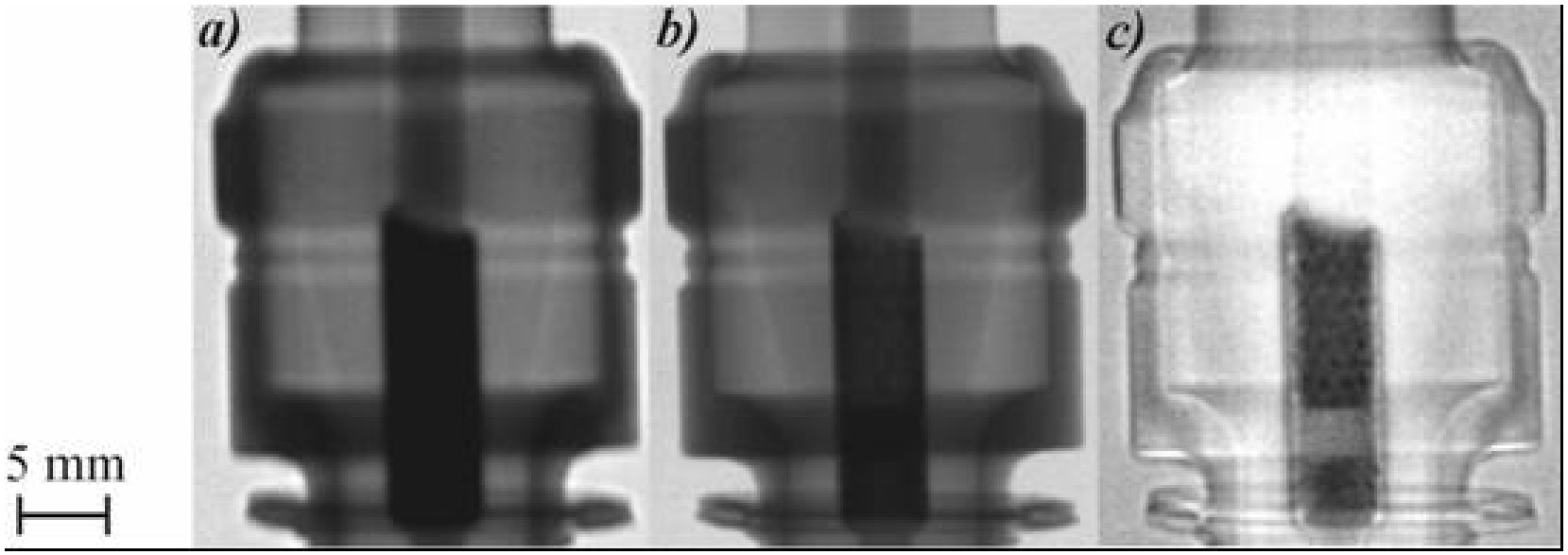

Image at: 6.9Å 3.2Å division

→ Steel becomes transparent, electrodes more clearly visible

The Neutron Radiography Station NEUTRA for thermal neutrons

X-ray option

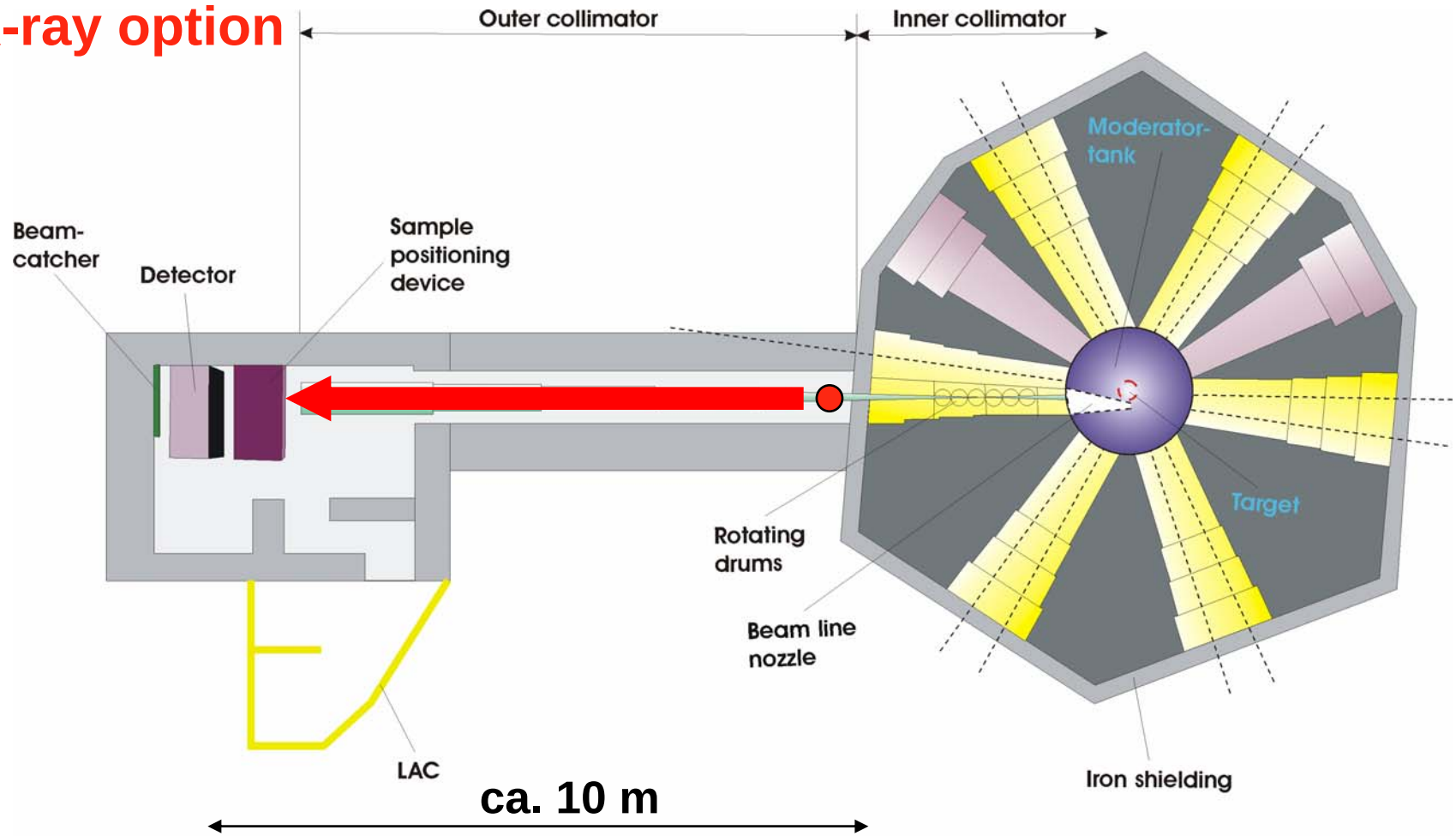

Example for a comparison

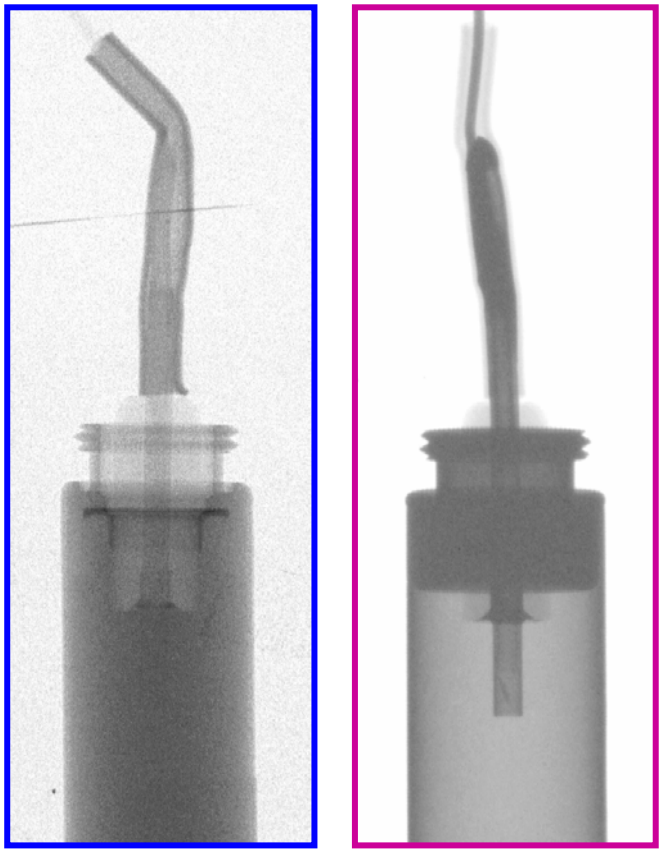

neutron X-ray

End-connector of a He-3 counter

measured with Imaging Plates under similar conditions

- Check of the He-3 gas content with n
- Status of the wire connection with X

Applications of neutron imaging

(selected cases)

- All cases where organic liquids are involved
- Adhesive connections, especially in metals
- Explosives detection
- Inspection of nuclear fuel
- Hydride accumulation, corrosion of metals
- In-situ diagnostic of processes, e.g. electric fuel cells
- Analysis of museums objects (unique samples!)
- Biologic tests (in-situ root growing)
- Standard NDT (turbine blades, casting pieces, …)

Inspection of a motorcar door with neutrons

photograph

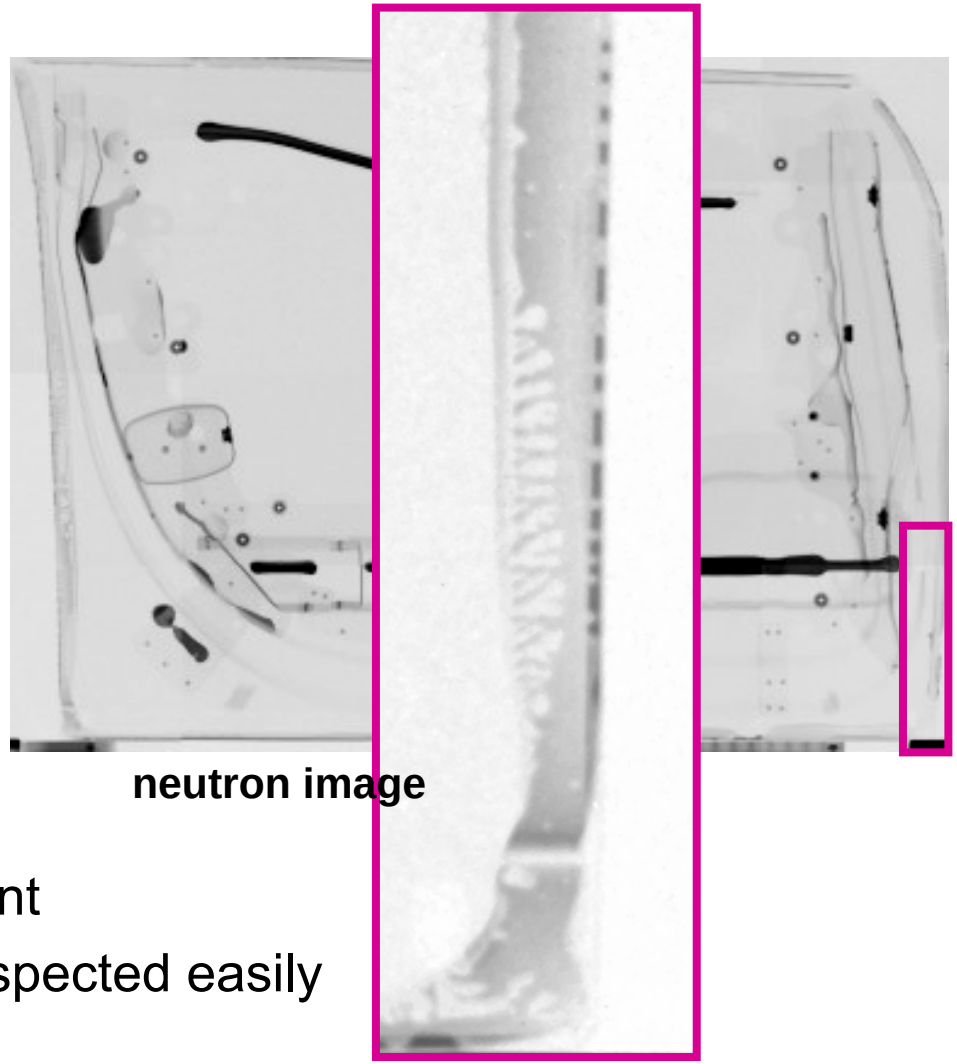

neutron image

- the metallic parts are transparent
- the adhesive bounds can be inspected easily

Determination of the U-235 content (enrichment) in nuclear fuel elements

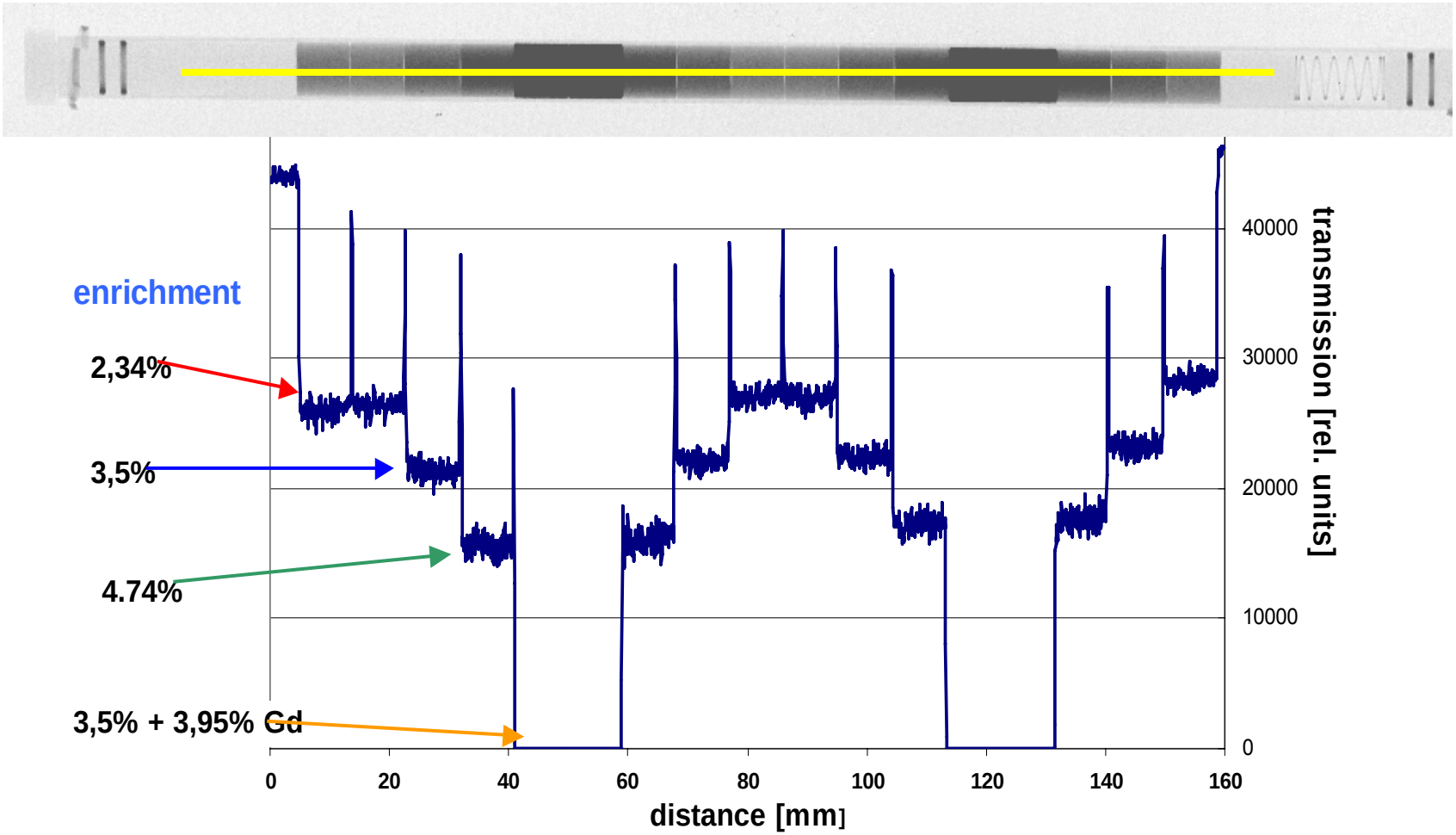

“Mercur from Uster”

Roman bronze sculpture

Taken from the Swiss National Museum, Zurich

Due to the high *lead content*, neutron imaging is advantageously applied

Facility utilization NEUTRA 2004

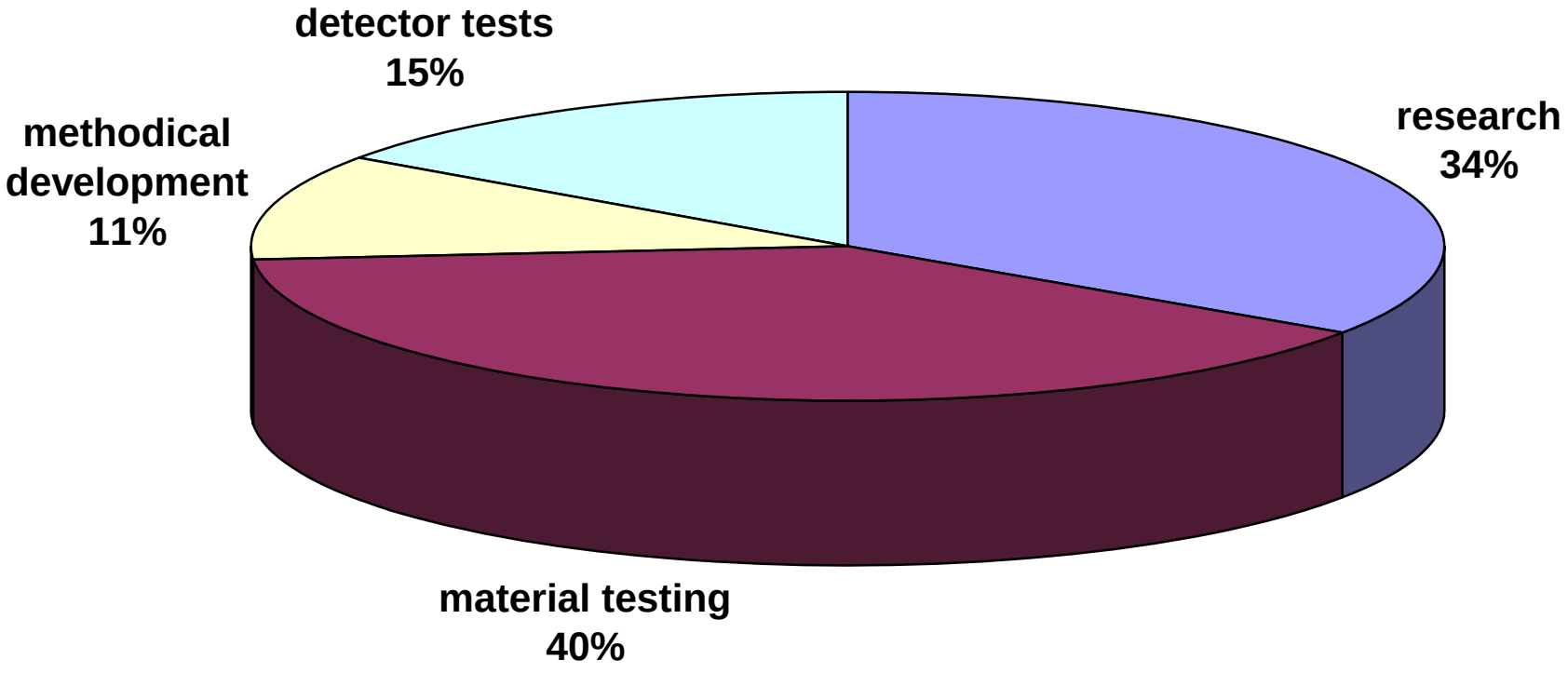

Methods

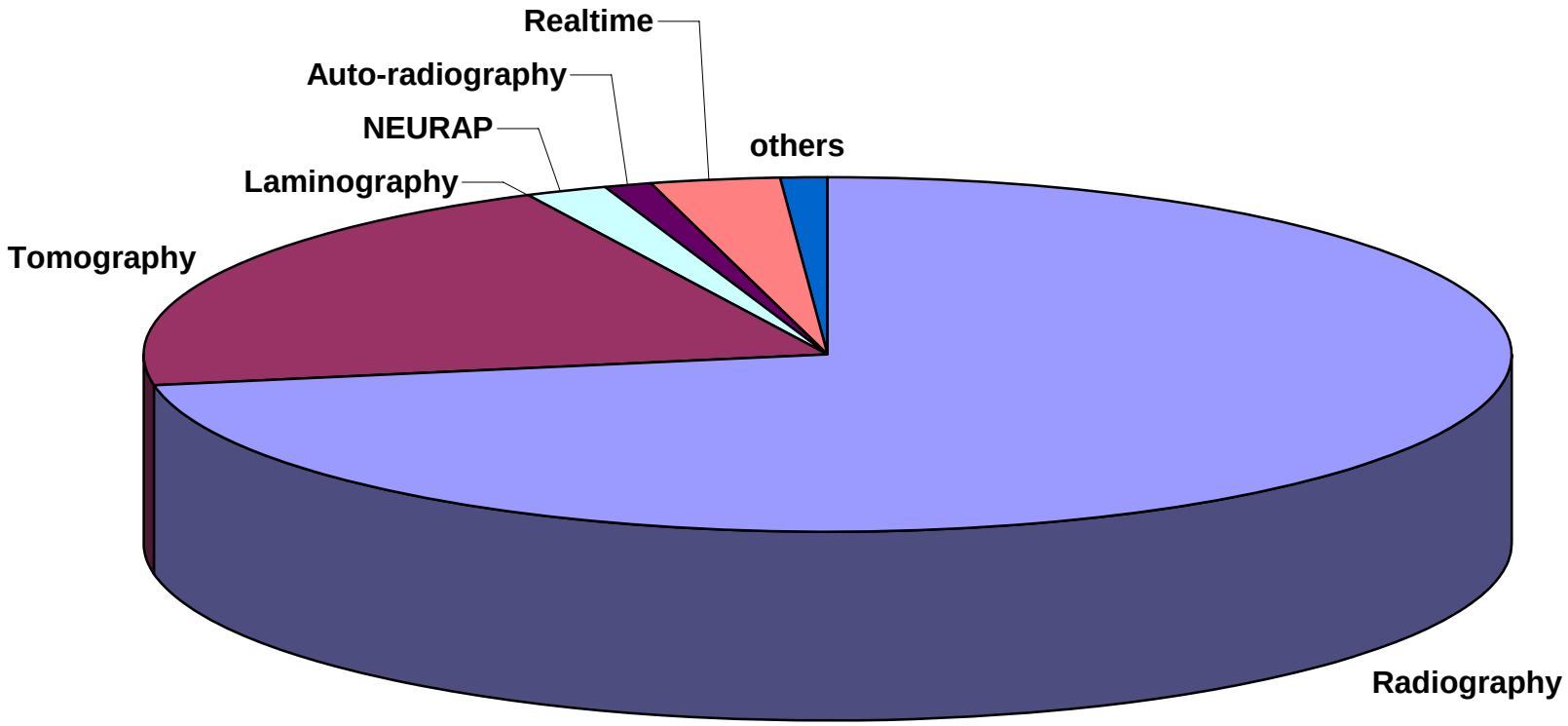
Realtime
Auto-radiography
NEURAP
Laminography
Tomography
others
Radiography

Detectors

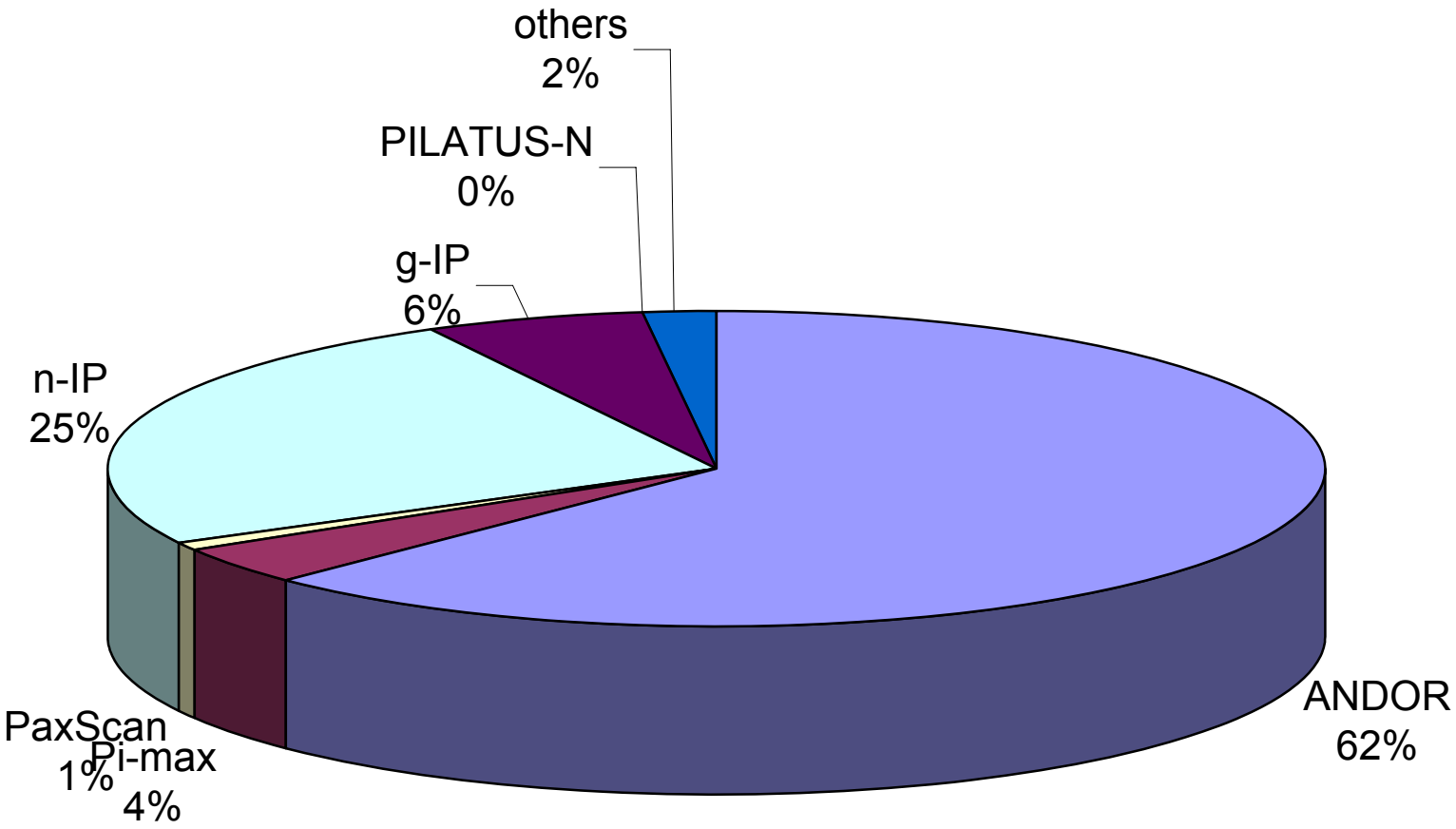

User countries

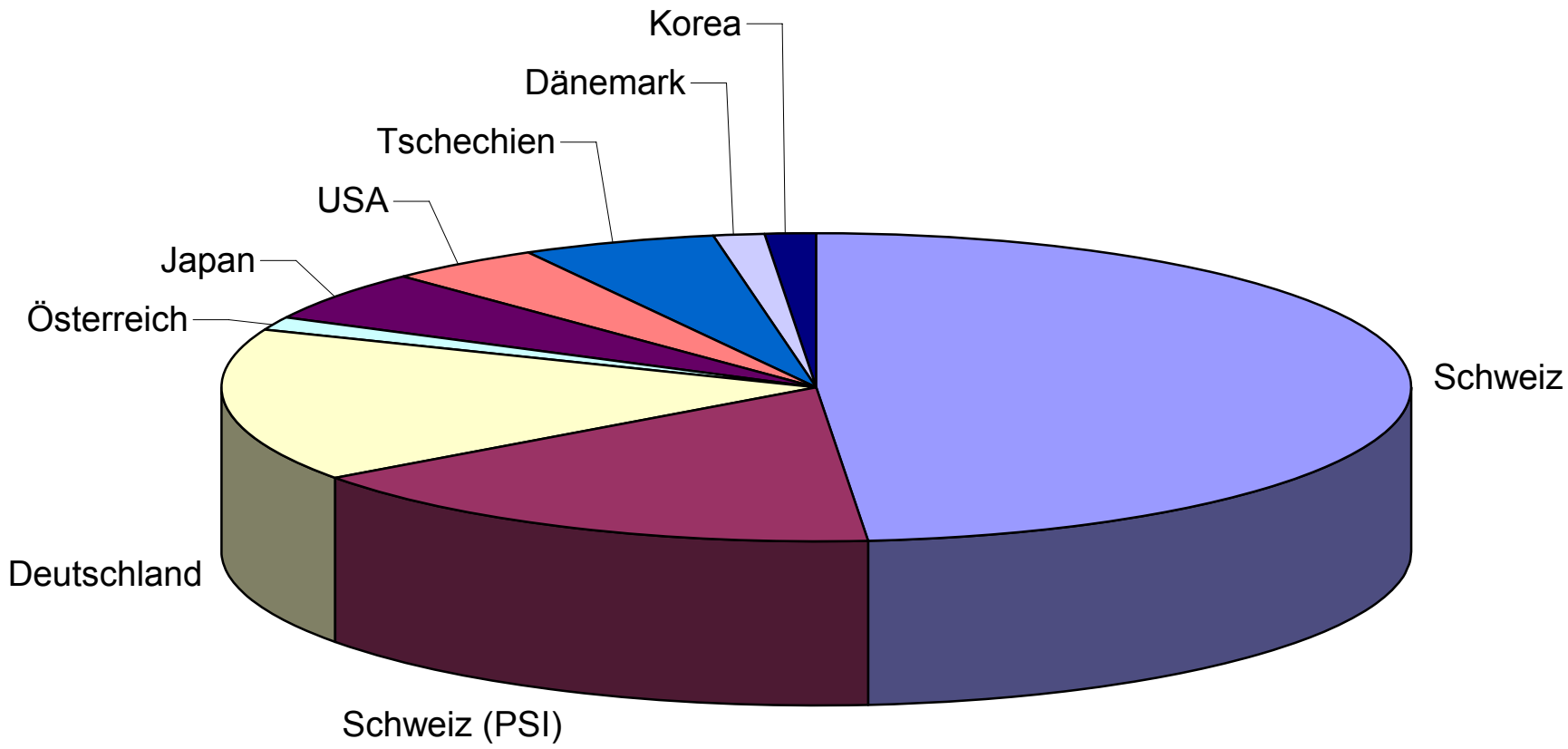

Without any user support for traveling and accommodation until now!

Conclusions

- Neutron imaging methods are **established** at PSI and used for many interesting applications in science and technology
- There has been a strong **progress on the detector side** which makes the method more attractive and diverse in applications
- There is potential for several **new options** to improve the methodology (especially at new sources)
- An **easy access** to the facility will help to attract industrial (commercial) partners
- A **network** of the NR facilities will improve the flexibility and the interaction between the partners, maybe with the help of NMI3!?

Further information can be found at:

http://neutra.web.psi.ch/